



# HHS Public Access

Author manuscript

*J Pathol.* Author manuscript; available in PMC 2024 July 30.

Published in final edited form as:

*J Pathol.* 2024 March ; 262(3): 271–288. doi:10.1002/path.6238.

## Image-based multiplex immune profiling of cancer tissues: translational implications. A report of the International Immunology Biomarker Working Group on Breast Cancer

*A full list of authors and affiliations appears at the end of the article.*

### Abstract

Recent advances in the field of immuno-oncology have brought transformative changes in the management of cancer patients. The immune profile of tumours has been found to have key value in predicting disease prognosis and treatment response in various cancers. Multiplex immunohistochemistry and immunofluorescence have emerged as potent tools for the simultaneous detection of multiple protein biomarkers in a single tissue section, thereby expanding opportunities for molecular and immune profiling while preserving tissue samples. By establishing the phenotype of individual tumour cells when distributed within a mixed cell population, the identification of clinically relevant biomarkers with high-throughput multiplex immunophenotyping of tumour samples has great potential to guide appropriate treatment choices. Moreover, the emergence of novel multi-marker imaging approaches can now provide unprecedented insights into the tumour microenvironment, including the potential interplay between various cell types. However, there are significant challenges to widespread integration of these technologies in daily research and clinical practice. This review addresses the challenges and potential solutions within a structured framework of action from a regulatory and clinical trial perspective. New developments within the field of immunophenotyping using multiplexed tissue imaging platforms and associated digital pathology are also described, with a specific focus on translational implications across different subtypes of cancer.

### Keywords

multiplex immunofluorescence; multiplex immunohistochemistry; tumour infiltrating lymphocytes; multiplex imaging; digital image analysis; tumour immune profiling; cancer prognosis; therapy response; clinical integration

---

This is an open access article under the terms of the Creative Commons Attribution-NonCommercial-NoDerivs License, which permits use and distribution in any medium, provided the original work is properly cited, the use is non-commercial and no modifications or adaptations are made.

\*Correspondence to: A Rahman, UCD School of Medicine, UCD Conway Institute, University College Dublin, Belfield 4, Dublin, Ireland. arman.rahman@ucd.ie.

Author contributions statement

CAJ, AR, and WMG conceptualised, developed the methodology and wrote the original draft. DBP was also involved in writing. AR, WMG, and RS were responsible for conceptualising, designing, editing the article and supervising. All remaining authors have provided critical revisions and agreed to publish the final version of the manuscript.

## Fundamentals of immune infiltration in cancer

In earlier concepts of cancer, the specific role of the immune system in the pathogenesis of malignancy was not well recognised. Over the last 15 years, however, the crucial role that the host immune system plays in tumour evolution has been brought to the forefront of cancer research; indeed, the immune landscape of tumours has emerged as a key hallmark of cancer [1]. During oncogenesis, alteration of the tumour microenvironment (TME) and tumour neoantigens trigger signals that facilitate immune responses in an attempt to eliminate preneoplastic cells [2]. Immune cells of varying density can be found in most types of malignancy due to the immunogenic response triggered by cancer cells [3]. The accumulation of different immune cells can have both tumour-promoting and tumour-suppressive functions [4].

In the first phase of tumorigenesis, cytotoxic immune cells such as NK and cytotoxic CD8<sup>+</sup> T cells identify and kill only highly immunogenic cancer cells. Consequently, less immunogenic cells escape the reach of both the adaptive and innate immune systems, fostering the progression to malignancy [5]. Thus, heterogeneous populations of immune infiltrates can drive tumour progression via a complex network of crosstalk between themselves and the other components of the TME. The qualitative characterisation of this interplay between immune infiltrates and cancer cells is called the immune contexture [6], which encompasses the density of each immune infiltrate and their spatial architecture across the tumour. Profiling immune contexture is one of the most significant ways to obtain insights into immune responses and has the potential to provide information with predictive and prognostic value [6]. Numerous studies over the years have provided strong evidence linking the presence of tumour-infiltrating lymphocytes (TILs) with clinical outcomes in various tumour types, such as melanoma, breast, colorectal, and non-small cell lung cancer (NSCLC) [7–11]. Hence, there is considerable interest in the scientific community with respect to approaches that can appropriately profile the immune contexture in cancer tissue samples.

Routine H&E staining in diagnostic laboratories allows for histopathological assessment of the general degree of immune infiltration, but possesses significant limitations. Significantly, subtyping of functionally distinct immune cell populations is not possible with H&E staining. Even though the presence of a specific immune population is important, more nuanced characteristics, including the quantity, functional state, spatial distribution, and interplay of immune subpopulations in the TME, collectively influence tumour progression [12]. Therefore, mapping multiple layers of biological characteristics is required to acquire information of maximum clinical value. To achieve this, many state-of-the-art multiplexed imaging technologies have been developed in recent years [13]. These platforms offer the ability to quantitatively assess multiple biomarkers to elucidate the biological characteristics, density, and spatial distribution of different classes of immune cells with objective quantitative data. The ability to perform multiparametric assessment of immune cells allows one to explore and extract a plethora of novel spatial features of translational and functional significance.

## Advantages of multiplex immunostaining

Traditionally, H&E and conventional immunohistochemistry (IHC) have been considered the gold standard for evaluating histopathological biomarkers of clinical relevance. However, given that only a very limited number of markers can be assessed at the same time, such approaches can be extremely limiting. In the era of ever-increasing findings in immunoncology research, it is becoming more and more crucial to obtain information on multiple biomarkers to make more accurate clinical decisions [14]. It has already been shown in a meta-analysis that multiplex immunostaining-based assays outperform other commonly used assay modalities in predicting response to anti-PD-1/PD-L1 therapy, including PD-L1 IHC, tumour mutational burden, and gene-expression profiling [15].

Multiplex IHC and immunofluorescence (mIHC/IF) allow simultaneous analysis of multiple markers on the same tissue section. Depending on different mIHC/IF technologies, the number of assessable markers generally varies between relatively discrete panels (two to eight markers) (Figure 1) to high-plex panels (up to 100) [13]. Simultaneous assessment of multiple markers provides mIHC/IF with key advantages over H&E or conventional IHC. First, with conventional IHC, it is often necessary to stain the same number of serial tissue sections as the number of markers that need to be assessed, risking tissue depletion, particularly on core needle biopsies that are the mainstay of primary diagnosis in many settings (Figure 2). Indeed, with these traditional approaches it can be very challenging to investigate an extensive panel of immune markers after exhausting most of the usable sections for routine diagnostic markers. Second, it is only possible to visually cross-compare up to two or three consecutive sections if one wants to study the colocalisation or spatial relationship between different markers. For example, an average lymphocyte is 10  $\mu\text{m}$  in diameter, and with sections of standardised thickness (3–5  $\mu\text{m}$ ), it is possible to have a maximum of three consecutive sections of the same cell [13]. Alternatively, there is an option to use virtual multiplexing, where multiple single-stained serial images are digitally stacked on top of one another to provide a multiplex effect [16]. However, these images are not always reliable for cell phenotyping, especially where there are co-expressed markers, due to the similar limitation in that specific cells are not consistently present across multiple tissue sections. Also, these workflows are impractical for most high-throughput clinical study/trial requirements [17].

As far as biological information is concerned, multiplex imaging brings a wealth of additional information to the table, which is impossible to extract from H&E or conventional IHC (Figure 3). The majority of methodologies described for TIL scoring in histopathological samples use H&E staining [18,19]. However, H&E staining only reveals the degree of total lymphocyte infiltration. TIL populations may contain both antitumour and tumour-promoting immune cells; therefore, without further subtyping, it is not possible to capture an accurate representation of the immune contexture. Multiplex imaging techniques offer a huge advantage here, as it is possible to simultaneously phenotype multiple immune populations. Admittedly, it is possible to quantify the infiltration of specific populations with single-plex IHC staining of serial sections, but in most cases it is not enough to characterise their functional status in samples. For example, T cell populations may be labelled with CD3. However, T cells can co-exist in dozens of different states having

significantly different biological functions in the TME, states that can only be characterised by further profiling the lineage markers in the cells. For instance, CD3<sup>+</sup>CD8<sup>+</sup> co-expressing T cells represent cancer-killing cytotoxic T cells and CD3<sup>+</sup>CD4<sup>+</sup>FOXP3<sup>+</sup> co-expressors represent tumour-promoting T regulatory cells (Tregs).

Furthermore, multiplex staining provides a much deeper insight into the spatial characteristics of the targeted cell populations and allows any proximal association between cells expressing specific markers to be deciphered. Assessment of immune cells in a multiplex setting enhances spatial mapping of immune cells in relation to tumour cells as malignant cells can be labelled concurrently [20]. Combined with digital image analysis (DIA), this process allows faster and higher-throughput quantification of stromal, intratumoural, and peritumoural TILs compared with manual evaluation.

## DIA and artificial intelligence

In a multiplex-based immune profiling workflow, the first step after staining involves digitising the stained section into a high-resolution image using a whole-slide imaging scanner. Multiplex images carry a massive amount of complex biological information, and to extract and manage this wealth of data, histopathological DIA software is used.

Prior to analysis, raw scan images usually undergo a number of preprocessing steps to eliminate autofluorescence and unmix overlapping fluorophore signals. The image analysis workflow for immune profiling in tumour tissue primarily involves three steps (Figure 4). In the first, tissue segmentation is performed, and involves the automated identification and partitioning of separate tissue compartments, such as tumour and stroma [21]. Tissue segmentation can also be carried out by manually annotating regions of interest (ROIs), especially in studies with fewer samples. However, in multiplex studies, an epithelial marker, like cytokeratin, is generally used to assist the software in segmenting tumour and stromal content in the tissue [22]. This streamlines and increases the efficiency of quantifying intratumoural and stromal TILs in a large number of tissue samples. The second step is cell segmentation, where each cell in the tissue is detected and segmented by the software, typically based on a nuclear counterstain such as DAPI. However, studies have shown that using signals from multiple markers, including membrane markers, significantly improves cell segmentation compared with single markers or counterstaining [23,24]. Following cell segmentation, each cell is phenotypically classified according to single or multiple markers. Cell or object classifying tools mainly fall into two categories. Threshold-based classifiers determine if a cell is positive or negative for a marker depending on the signal intensity. Artificial intelligence (AI)-based classifiers are algorithms that are trained by a user on a variety of staining and morphological features to detect specific objects/cells of interest. Post-training, they automatically perform object segmentation on the samples. AI-based classifiers allow the incorporation of the domain-specific knowledge of experienced pathologists in developing the image analysis algorithm. Generally, pathologists or specialists train these kinds of classifier by manually annotating objects, tissue, or different morphological and biological structures. Pathologists feed the algorithm such data until the classifier learns to distinguish objects with acceptable proficiency. This offers a much more rapid, unbiased, and potentially accurate assessment of features of interest.

In immuno-oncology research, AI classifiers are now widely employed for tissue segmentation and lymphocyte detection within the context of H&E-based images [25–27]. In multiple key studies, AI-based approaches have shown a better or similar level of accuracy compared with expert pathologists [28,29]. AI algorithms are increasingly being integrated into multiplex image analysis workflows to improve structure and object identification and phenotypic segregation [30,31]. Due to tissue heterogeneity, phenotyping of simple objects becomes troublesome if the classifier only works with a few basic parameters, such as signal intensity or cell diameter. AI-based semi-automated or automated image analysis approaches are very useful in those scenarios. As the AI-based classifiers can be trained over a wide variety of tissue samples and utilise large datasets, the classifiers are able to gather a lot more information to identify specific morphological features. Zarubin *et al* [31] trained an AI algorithm on 219 manually annotated regions from different tissues (kidney, ureter, lung, ureter, lymph node, tonsil) and showed near human accuracy in segmenting various cell types (tumour, immune) in multiplexed images. For chromogenic mIHC, it is challenging to digitally evaluate more than four biomarkers in the same section due to a lack of readily available analysis tools. To solve this, Fassler and colleagues [32] developed two complementary deep learning-based tools (*Color AE* and *U-Net*) utilising pathologist annotations and constructed an ensemble method that reliably classified six distinctly chromogenically labelled immune populations.

After cell segmentation and phenotyping, the final analysis involves profiling the spatial architecture of the markers. With cell segmentation, DIA software can create a topographical map of every cell in the tissue using the individual cell coordinates [33]. Based on those data, any spatial feature of each cell phenotype can be analysed, and potential clinically significant associations can be assessed further. Currently, there are multiple high-end commercial and open-source DIA software packages that offer both AI- and non-AI-based analysis tools (listed in [34]).

## Pitfalls of multiplex immunostaining

Multiplexed staining assays are unique sample-sparing tools that offer a superior histopathological interpretation of disease heterogeneity compared with conventional staining techniques. Nevertheless, they come with certain methodological pitfalls that should be considered before designing any experiment. In general, multiplex immunostaining workflows are more technically challenging and time-consuming. Compared with classical IHC, it involves a greater number of experimental variables and thus requires a more comprehensive and lengthy optimisation process.

Any IHC technique requires extensive validation of antibody specificity and optimisation of their staining conditions. In order to develop a mIHC/IF panel, the staining conditions for each antibody need to be further optimised in a multiplexed setting [35]. Comparison with standard single-plex IHC/IF represents the gold standard during this optimisation. Staining markers in the correct sequence can be critical, as changes in tissue antigenicity during multiple staining rounds can affect antibody performance. Simultaneous staining of multiple targets on the same tissue sample introduces additional complexities. For example, staining multiple targets with fluorophores having close spectral emission poses the risk of spectral

overlap. This may lead to fluorophore signals leaking into the wrong channel and resulting in false-positive detections. Thus, variables such as reagent concentrations, antibody–dye pairing, and the antibody staining sequence in the panel must be thoroughly optimised to prevent spectral overlapping and accurate detection of targets. Parra *et al* [36] provided a detailed discussion on the procedural requirements and a step-by-step guideline for proper optimisation of a mIF staining panel. Some vendors now provide spectral unmixing tools in their DIA packages that can eliminate overlapping signals during post-processing of raw images [35]. Using these tools, users can build spectral libraries by profiling the exact emission spectrum of individual fluorophores. These libraries are then used to deconvolute overlapping signals. IF-based techniques are also inherently susceptible to issues related to autofluorescence, which can interfere with the detection of targets labelled with fluorophores that emit at wave-lengths near the autofluorescence emission spectrum. These issues can be reasonably resolved by following an optimal protocol for handling pre-analytical conditions, like tissue fixation and sample preparation, then removal of autofluorescence signal in the scanned images through DIA unmixing tools [35]. Additionally, multiple antibodies targeting closely spaced epitopes may create steric hindrances and impede antibody binding [37]. Adequate stripping of antibodies after each staining cycle is necessary to prevent this.

Together, the use of multiple antibodies, high-end equipment, and DIA packages makes multiplex staining considerably costlier than traditional IHC, particularly for high-throughput studies. Consequently, for most immune profiling studies with large sample sizes, tissue microarrays (TMA) are used instead of full-face sections. However, in some cases, tissue cores in a microarray may not adequately represent the heterogeneity of marker expression in the sample [38,39]. Some immune populations are often dispersed irregularly across tumour sections; thus, small-sized tissue cores are often not sufficient to capture the accurate spatial composition of the populations [40]. For similar reasons, TMAs are also unlikely to be ideal for profiling rare immune populations and spatial phenotypes. Several validation studies suggest that increasing the number of cores and carefully selecting cores that are more representative of the marker distribution leads to an improvement in the concordance between TMA cores and full-face sections, particularly for markers that are preferentially distributed [41,42].

## Statistical considerations for multiplex immune profiling

mIHC/IF assays generate high-resolution, single-cell spatial data, usually spanning thousands of observations per sample across multiple ROIs. Each observation contains information on cellular phenotype, protein expression, and spatial location. Due to the complex and hierarchical nature of these data, statistical methods must be carefully vetted to minimise bias and maximise knowledge learned. One inherent challenge of immune profiling with mIHC/IF is intratumoural heterogeneity, whereby immune cell densities and/or protein levels can vary dramatically across ROIs within a single tumour sample [43–45]. This variation can be either random or related to anatomic features, such as the invasive tumour margin [46,47]. Without a standardised approach for analysing mIHC/IF data, heterogeneity increases the risk of bias and/or inter-observer discordance [43]. A customary statistical method to overcome heterogeneity is to sample tumours across multiple high-powered fields/ROIs, and to report outcomes as the mean of these ROIs [43]. This approach



is simple and effective, and is the basis for clinically validated prognostic instruments, such as the breast cancer H&E stromal TIL score (which relies on whole-slide visual averaging) [19,43] and the colon cancer Immunoscore (which relies on averaging cell counts across four distinct spatial/cellular compartments) [48,49].

The process of averaging estimates across numerous high-powered fields requires significant manual and computational labour; therefore, it is of practical interest to ascertain how many ROIs must be sampled to overcome the effects of intratumoural heterogeneity. Recently, mIF data from a breast cancer preoperative immunotherapy clinical trial were used to characterise the impact of ROI sample size on statistical power [50]. Using bootstrapping simulations to emulate 1,000 trials under various ROI sample sizes, it was shown that undersampling of ROIs resulted in unstable estimates of treatment effect, whereas sampling of 15 or more ROIs per specimen resulted in consistent estimation of treatment effect. In addition to ROI sample size, the spatial location of sampled ROIs may also influence the estimation of mIHC/IF results. For example, acknowledging the natural inclination of immune cells to cluster at the invasive margin, oversampling of ROIs at the invasive margin relative to other areas would have the effect of inflating the cell density estimate of a given tumour. Statistical methods could be used to adjust estimates of the mean for anatomic confounders such as the invasive margin. Linear regression modelling could be employed, with the inclusion of spatial covariates into the model to account for proximity to the invasive margin, thus generating estimates of mean immune cell density that are independent of sampling effects of the invasive margin. In relation to the Immunoscore used in colon cancer, a similar but less statistically formalised method is employed, whereby CD3 and CD8 counts are estimated across each of two tumour compartments (invasive edge and tumour), and then averaged [49].

Finally, mIHC/IF output images bear an uncanny resemblance to topographical maps, with tumour epithelial nests and other anatomic structures mimicking geographical features (such as polygonal boundaries of continents), and immune cell locations representing spatial point locations of features on the map (such as locations of cities). As such, another promising direction is to use abundant spatial statistical techniques and software packages (e.g. Spatstat) borrowed from the fields of geography and ecology [51]. Using these programs, one can convert mIHC/IF output data into vector-format datasets that overlay immune cell location (spatial points) with anatomic feature location (spatial polygons). Software can then be used to estimate cell densities at the local level (across partitioned regions of an ROI), and to formally interrogate the relationship between cell location/density, the surrounding microanatomy, and neighbouring cells. It is of paramount importance to tackle such analyses using a multidisciplinary approach, whereby immunologists, pathologists, and statisticians work together to ensure proper hypothesis generation, histological annotation, and statistical modelling/testing. For detailed information on analysing and reporting spatial immune profiling data, please see the companion manuscript from The International Immuno-Oncology Biomarker Working Group [52].

## Clinical and translational implications of tissue-based immune profiling in cancer

The remarkable success of immunotherapy, particularly the checkpoint inhibitor therapeutic strategies targeting CTLA-4 and PD-1/PD-L1, has revolutionised treatment for several types of malignancy, as well as our broader understanding of the clinical significance of immune contexture in cancer. Over the last couple of decades, numerous studies have confirmed the ability of tumour immune composition to significantly influence clinical outcomes in various cancer types [53]. This highlights the potential importance of immune profiling as a metric to be reported and used in clinical settings for tumour characterisation and for guiding clinical decisions.

A seminal study on colorectal cancer showed that the composition of TIL infiltrates is a better predictor of survival than routine TNM (tumour, node, metastasis) classification [10]. This finding first challenged the concept of only looking at neoplastic cell characteristics for assessing the risk of progression. Galon *et al* [54] developed the Immunoscore, which assigns a score of 0–4 based on the density of CD3<sup>+</sup> and CD8<sup>+</sup> populations in both the tumour centre and invasive margins [55]. Immunoscore correlates with disease-free and overall survival in colorectal cancer and other tumour types, including melanoma, breast, kidney, and lung cancers [56,57].

The efficacy of different forms of immunotherapy is critically affected by the immune composition of tumours before therapy [58] and the absence of T cells and tumour-specific T cell responses are key contributors to poor clinical responses [59]. These findings led to classifying immune composition in the TME into distinct phenotypes that correlate with patient responses to immunotherapy and prognosis. Several years of IHC-based spatiotemporal studies across different tumour types have established distinct immune phenotypes: hot tumours (immune-inflamed) and cold tumours (immune-excluded and immune-desert) [60]. The immune-inflamed phenotype is characterised by substantial infiltration of TILs in the tumour centre. It is associated with the presence of CD4<sup>+</sup> and CD8<sup>+</sup> T cells in the tumour parenchyma that reflects a preceding antitumour response mediated by an immune-permissive microenvironment. The immune-excluded phenotype is characterised by pronounced infiltration of immune cells localised at the tumour interface with surrounding tissue, instead of within the tumour centre. This class of tumour is hypothesised to be poorly immunogenic. The final phenotype, immune-desert tumours, is characterised by the absence of pre-existing T cells in either tumour parenchyma or stroma. These features indicate the absence of pre-existing antitumour immunity. Tumours with immune-desert phenotypes often exhibit poor response to immunotherapy [61].

Currently, with the ongoing discovery of these complex phenotypes of clinical significance, spatiotemporal multi-marker assessment of immune contexture is becoming a necessity in immune-oncology research. Hence, tissue-based multiplexing has evolved into an optimal investigating tool for identifying predictive and prognostic immune biomarkers [55]. A comprehensive list of studies focusing on the clinical relevance of immune profiling through mIHC/IF techniques is presented in Table 1.



## Cancer prognosis

The major fraction of immune infiltrates in cancer is comprised of T cells. T cell infiltration has been associated with survival outcomes in multiple different tumour types, including melanoma, breast, lung, colon, liver, and bladder [11,54,81–83]. CD8<sup>+</sup> cytotoxic T cells are widely regarded as the central players in antitumour immunity, and a higher degree of CD8 infiltration is mostly associated with favourable clinical outcomes [84–87]. CD4<sup>+</sup>FOXP3<sup>+</sup> Treg cells are critical subsets of helper T cells that suppress the antitumour immune response [88]. Recently, relatively small multiplex panels (three to four markers) are increasingly used to study T cell composition and their prognostic relevance in various cancers. Yamagami *et al* [67] assessed the composition of CD4<sup>+</sup>, CD8<sup>+</sup>, and Treg cell populations in endometrial cancer with mIF and found that patients with high Treg counts and Treg/CD8 ratios experience significantly worse survival. Several studies in different cancer types have shown that T cell aggregation in intratumoural regions was linked to better prognosis [10,66,89]. Spatial analysis of eight distinct immune subpopulations in pancreatic ductal adenocarcinoma with mIF found intratumoural T cell infiltration to be independently correlated with favourable patient survival [90]. In a similar study of NSCLC, cytotoxic T cell (CD3<sup>+</sup>, CD8<sup>+</sup>) infiltration was mapped using a multiplex panel and a higher level of intratumoural CD8<sup>+</sup> cell infiltration independently correlated with better survival [69]. Another recent study of NSCLC showed increased CD8<sup>+</sup> T cell density in the invasive margin to be positively associated with recurrence-free survival [91].

mIHC/IF assays are also widely used by researchers to study proximal associations between cancer and immune markers, as well as among different immune cell subtypes [92]. The proximity of malignant cells to specific immune subsets can suggest an effective antitumour or tumour-promoting environment that may be important for determining prognosis. Nearchou *et al* [93] simultaneously assessed the distribution of T cell infiltrates in intratumour locations and at invasive margins within the context of tumour budding in colorectal cancer. The study not only confirmed T cell infiltrates and tumour budding to be independent prognostic factors, but also found that the spatial relationship of lymphocyte infiltrates and tumour budding offers additional prognostic value. Combining all the features together into a prognostic index generated improved prognostic stratification for patients compared with any of the features individually. Another study explored the spatial relationship of 17 distinct leukocyte lineages with a 29-plex mIF platform. They found that the proximity of Treg and myeloid cells to tumour cells had a strong correlation with earlier cancer recurrence [94]. Similar results by multiplexing were also found in lung cancer and head and neck squamous cell carcinoma, where the proximity of Treg cells to carcinoma cells was linked to poor prognosis [91,95].

Together with T cell subsets, recent research has also highlighted the prognostic utility of other immune populations, such as B cells, macrophages, and dendritic cells. A recent study used multiplex staining for immune profiling of colon cancer and developed a highly prognostic signature comparable with the Immunoscore by combining the prognostic features of CD8<sup>+</sup> T cells and CD68<sup>+</sup>/CD163<sup>+</sup> macrophages. The signature further demonstrated significant prognostic efficacy in four other cancer types – oesophageal adenocarcinoma, bladder cancer, lung adenocarcinoma, and melanoma [96]. Multiplex

immunostaining techniques also allow identifying complex phenotypes, such as tertiary lymphoid structures [97,98]. Tertiary lymphoid structures are ectopic lymphoid structures of cellular aggregates, generally comprised of a germinal core with proliferating B cells and follicular dendritic cells, surrounded by a CD3<sup>+</sup> T cell zone [99]. The prevalence of tertiary lymphoid structures in tumours is generally suggestive of strong tumour immunity and is mostly correlated with a better prognosis [100].

## Predictive tool for therapy response

PD-L1 is the most well-studied and well-accepted predictive biomarker in the clinical setting for immune therapies. IHC-based PD-L1 assays have already been approved as companion diagnostic testing for selecting patients to receive checkpoint blockade therapies in several different cancer types [101,102]. However, PD-L1 alone has not been sufficient for optimal patient stratification [103] and several other components of the TME appear to affect the likelihood of therapy response. Strong evidence from multiple studies suggests that TIL infiltration with a T cell-inflamed phenotype is associated with an anti-PD-L1 therapy response [104]. In mismatch repair-proficient colorectal cancer CD8<sup>+</sup>PD-1<sup>+</sup> T cell infiltration was found to be the only biomarker predicting response to neoadjuvant immunotherapy [105]. De Vries *et al* [106] demonstrated evidence of  $\gamma\delta$  T cells contributing to an immune checkpoint blockade response in HLA class I-negative mismatch repair-deficient colon cancer patients. Multiplex immunostaining assays can serve as an ideal diagnostic tool to assess these kinds of complex immune subset in clinical settings.

When CD8<sup>+</sup> T cell distribution was assessed in melanoma TME, high CD8<sup>+</sup> cell density at the invasive margin was found to be associated with anti-PD-L1 therapy response [107]. In another recent mIF-based study with melanoma samples, spatial interactions between T cell populations and malignant cells were investigated, and higher CD8<sup>+</sup> cell density within close proximity to melanoma cells was found to be associated with a better response to anti-PD-1 therapy [72]. Interestingly, in Merkel cell carcinoma, the proximal association between PD-1 and PD-L1 was found to be predictive of an anti-PD-1 response [108].

In addition to predicting therapy response in patients using tissues sampled prior to therapy, immune profiling of early on-treatment patient biopsies has also been found to be very effective in predicting long-term therapy response. A multiplexed immune profiling study in a cohort of melanoma patients treated with combined CTLA-4 and PD-1 blockade therapy showed increased accumulation of CD8<sup>+</sup> cells in the tumour centre that was significantly correlated with the therapeutic response [109]. All of these studies support the clinical value of TIL profiling, and PD-L1 as a companion diagnostic test, with better predictive accuracy. As IHC-based techniques are already routinely used for clinical assays, tissue-based multiplexed platforms will be ideal tools for combining TIL scores with PD-L1 data. Similar strategies should also be adopted for designing immunotherapy clinical trials. This is crucial, as patient selection for clinical trials is still based on conventional toxicity and efficacy patterns observed with chemotherapy and targeted agents [110]. Very few clinical trials are adopting standard immune biomarkers for patient selection, which is a major impediment to proper characterisation of the biological response.

Apart from modulating the tumour response for immunotherapy, the immune composition of the TME has also been found to heavily influence the clinical outcome of other kinds of cancer treatment [111–113]. It was originally thought that chemotherapy only had an immunosuppressive effect. However, recent studies have shown that certain types of chemotherapy can facilitate an antitumoural immune response by inducing tumour-associated neoantigen expression [114]. Parra *et al* [75] investigated the change in immune composition after neoadjuvant chemotherapy (NAC) in tumour tissues from 112 NSCLC patients using two different six-plex IF panels to quantify 12 tumour-associated immune phenotypes. Higher levels of PD-L1 with T cell and tumour-associated macrophage cell infiltration were observed in samples from patient treated with NAC compared with those who had not received NAC, indicating that NAC induces a discrete immune response. Moreover, patients receiving NAC who had higher levels of helper T cells and tumour-associated macrophages showed better survival. In a similar study of HER2-positive breast cancer patients, an assessment of CD8<sup>+</sup> cells together with PD-L1 was found to be valuable in predicting the response to anti-HER2 neoadjuvant therapy [115].

### Implementing mIHC/IF technologies in daily clinical practice

Although multiplex imaging technologies have critical utility in clinical research, very few of these technologies have been adequately validated for clinical application. To date, no multiplex staining assays have been approved by the Food and Drug Administration for use in clinics as *in vitro* diagnostics [116]. With the growing need to better understand the TME for clinical decision-making, incorporating these technologies into clinical pathology is becoming increasingly necessary. There are several challenges to overcome for mIHC/IF techniques to become widely adopted in clinics.

To begin with, there are extensive infrastructure requirements to facilitate mIHC/IF and digital pathology in a clinical institution. In general, mIHC/IF images are composite files of separate images generated for each marker, creating a large file size. With a moderate-sized panel (five to seven markers), the whole-slide image size will probably fall between 0.5 and 4 gigabytes [117]. Consequently, a hospital will generate hundreds of terabytes of imaging data each year, and it is essential to have access to infrastructure that can store, process, and facilitate the sharing of this amount of data. Additionally, AI-based quantitative and spatially resolved image analysis of these images requires expensive high-end work-stations with powerful graphics processing units [118]. It also requires additional human resources with considerable statistical and bioinformatic expertise for downstream statistical analysis and robust data interpretation.

In addition to infrastructure requirements, ensuring consistency of these new mIHC/IF techniques by standardisation is also a critical impediment to their integration into clinics. Most mIHC/IF techniques are specific in their methodology, having unique staining and imaging platforms, different analysis packages, and image formats [13]. These factors inherently introduce variability, which raises the question whether data from independent laboratories can be compared.

In order to meet these challenges, The Cancer Immune Monitoring and Analysis Center (CIMAC) conducted a multistep harmonisation study to compare assay performance among independent laboratories and to determine whether it is feasible to generate comparable data regardless of the platform and site [119]. They have compared the staining of a five-marker immune panel (PD-L1, PD-1, CD3, CD8, and PanCK) on head and neck tumour samples among three different institutions using two different multiplexed imaging platforms – a mIF-based tyramide signal amplification system and chromogenic mIHC. Both platforms were evaluated for sensitivity, specificity, and reproducibility, followed by the harmonisation of three aspects – staining, image acquisition, and image analysis procedures across the two platforms. Post-harmonisation of the data, for most markers, the correlation coefficient exceeded 0.85; combining all markers, it was over 0.7, with a median coefficient of variation below 0.1, indicative of excellent precision between measurements. These findings demonstrated that despite differences in protocols, platforms, reagents, and image analysis applications, independent multiplex immunostaining platforms could produce harmonised data without imposing rigid standardisation.

One of the significant factors that affected the harmonisation effort was pre-analytical variables, such as sample procurement and processing. It is generally recognised that pre-analytical variables pose challenges to IHC standardisation [120,121]. Thus, CIMAC has formulated an ‘umbrella’ protocol for standardising pre-analytical conditions, which can be adopted to minimise analytical variability across laboratories [122]. They are also putting considerable effort into analytically validating assay platforms based on their ability to perform the most robust and unbiased analyses, allowing them to prioritise specific assays for clinical trials.

A six-institution intrasite collaboration in 2019, termed the MITRE study, developed a standardised end-to-end workflow for a six-plex mIF assay (PD-L1, PD-1, CD8, CD68, FOXP3, and CK) suitable for multisite trials [123]. Assay optimisation led to sensitive and reproducible results between and within all sites. Further similar efforts must be made to address standardisation issues with mIHC/IF. The Society for Immunotherapy of Cancer (SITC) has taken a crucial step in that direction by forming a 21-member task force of pathologists and research leads from academia and pharmaceutical companies to develop best practice guidelines for optimising and validating multiplex immunostaining assays [37]. Overall, for validating these multiplex imaging assays, a harmonised, systematic approach should be designed and adopted for clinical use. Throughout the process, there needs to be more collaboration between the clinical and scientific communities. To meet high infrastructure requirements, solutions like cloud-based analysis pipelines can be adopted as an alternative to developing storage and analysis infrastructure in hospitals. This will enable easy access to the heavy computational requirements and facilitate collaboration among researchers and pathologists by providing shared access to data and algorithms. In addition, there should be free public databases for multiplexed images, with widely accepted minimum information standards [124]. This will encourage meta-analyses and help to develop more reliable algorithms. Ultimately, the future adoption of multiplex imaging technologies in clinics will require more harmonisation, standardisation, and validation studies addressing all the factors contributing to variability. This will not only ensure

improved accuracy and reproducibility of immune profiling, but also facilitate a faster and more streamlined process of test development.

## Authors

Chowdhury Arif Jahangir<sup>1</sup>, David B Page<sup>2</sup>, Glenn Broeckx<sup>3,4</sup>, Claudia A Gonzalez<sup>1</sup>, Caoimbe Burke<sup>1</sup>, Clodagh Murphy<sup>1</sup>, Jorge S Reis-Filho<sup>5</sup>, Amy Ly<sup>6</sup>, Paul W Harms<sup>7</sup>, Rajarsi R Gupta<sup>8</sup>, Michael Vieth<sup>9</sup>, Akira I Hida<sup>10</sup>, Mohamed Kahila<sup>11</sup>, Zuzana Kos<sup>12</sup>, Paul J van Diest<sup>13,14</sup>, Sara Verbandt<sup>15</sup>, Jeppe Thagaard<sup>16,17</sup>, Reena Khiroya<sup>18</sup>, Khalid Abduljabbar<sup>19</sup>, Gabriela Acosta Haab<sup>20</sup>, Balazs Acs<sup>21,22</sup>, Sylvia Adams<sup>23,24</sup>, Jonas S Almeida<sup>25</sup>, Isabel Alvarado-Cabrero<sup>26</sup>, Farid Azmoudeh-Ardalan<sup>27</sup>, Sunil Badve<sup>28</sup>, Nurkhairul Bariyah Baharun<sup>29</sup>, Enrique R Bellolio<sup>30</sup>, Vydehi Bheemaraju<sup>31</sup>, Kim RM Blenman<sup>32,33</sup>, Luciana Botinelly Mendonga Fujimoto<sup>34</sup>, Octavio Burgues<sup>35</sup>, Alexandros Chardas<sup>36</sup>, Maggie Chon U Cheang<sup>37</sup>, Francesco Ciompi<sup>38</sup>, Lee AD Cooper<sup>39</sup>, An Coosemans<sup>40</sup>, Germán Corredor<sup>41</sup>, Flavio Luis Dantas Portela<sup>42</sup>, Frederik Deman<sup>3</sup>, Sandra Demaria<sup>43,44</sup>, Sarah N Dudgeon<sup>45</sup>, Mahmoud Elghazawy<sup>46,47</sup>, Claudio Fernandez-Martín<sup>48</sup>, Susan Fineberg<sup>49</sup>, Stephen B Fox<sup>50</sup>, Jennifer M Giltneane<sup>51</sup>, Sacha Gnjatic<sup>52</sup>, Paula I Gonzalez-Ericsson<sup>53</sup>, Anita Grigoriadis<sup>54,55</sup>, Niels Halama<sup>56</sup>, Matthew G Hanna<sup>57</sup>, Apama Harbhajanka<sup>58</sup>, Steven N Hart<sup>59</sup>, Johan Hartman<sup>22,60</sup>, Stephen Hewitt<sup>61</sup>, Hugo M Horlings<sup>62</sup>, Zaheed Husain<sup>63</sup>, Sheeba Irshad<sup>64</sup>, Emiel AM Janssen<sup>65,66</sup>, Tatsuki R Kataoka<sup>67</sup>, Kosuke Kawaguchi<sup>68</sup>, Andrey I Khramtsov<sup>69</sup>, Umay Kiraz<sup>65,66</sup>, Pawan Kirtani<sup>70</sup>, Liudmila L Kodach<sup>71</sup>, Konstanty Korski<sup>72</sup>, Guray Akturk<sup>73</sup>, Ely Scott<sup>74</sup>, Anikó Kovács<sup>75,76</sup>, Anne-Vibeke Lænkholm<sup>77,78</sup>, Corinna Lang-Schwarz<sup>9</sup>, Denis Larsimont<sup>79</sup>, Jochen K Lennerz<sup>80</sup>, Marvin Lerousseau<sup>81,82,83</sup>, Xiaoxian Li<sup>84</sup>, Anant Madabhushi<sup>85</sup>, Sai K Maley<sup>86</sup>, Vidya Manur Narasimhamurthy<sup>87</sup>, Douglas K Marks<sup>23</sup>, Elizabeth S McDonald<sup>88</sup>, Ravi Mehrotra<sup>89,90</sup>, Stefan Michiels<sup>91</sup>, Durga Kharidehal<sup>92</sup>, Fayyaz ul Amir Afsar Minhas<sup>93</sup>, Shachi Mittal<sup>94</sup>, David A Moore<sup>95</sup>, Shamim Mushtaq<sup>96</sup>, Hussain Nighat<sup>97</sup>, Thomas Papatomas<sup>98,99</sup>, Frederique Penault-Llorca<sup>100</sup>, Rashindrie D Perera<sup>101,102</sup>, Christopher J Pinard<sup>103,104,105,106</sup>, Juan Carlos Pinto-Cardenas<sup>107</sup>, Giancarlo Pruneri<sup>108,109</sup>, Lajos Pusztai<sup>110,111</sup>, Nasir Mahmood Rajpoot<sup>112</sup>, Bernardo Leon Rapoport<sup>113,114</sup>, Tilman T Rau<sup>115</sup>, Joana M Ribeiro<sup>116</sup>, David Rimm<sup>117,118</sup>, Anne Vincent-Salomon<sup>119</sup>, Joel Saltz<sup>120</sup>, Shahin Sayed<sup>121</sup>, Evangelos Hytopoulos<sup>121,122</sup>, Sarah Mahon<sup>123</sup>, Kalliopi P Siziopikou<sup>124</sup>, Christos Sotiriou<sup>125,126</sup>, Albrecht Stenzinger<sup>127</sup>, Maher A Sughayer<sup>128</sup>, Daniel Sur<sup>129</sup>, Fraser Symmans<sup>130</sup>, Sunao Tanaka<sup>131</sup>, Timothy Taxter<sup>132</sup>, Sabine Tejpar<sup>15</sup>, Jonas Teuwen<sup>133</sup>, E Aubrey Thompson<sup>134</sup>, Trine Tramm<sup>135</sup>, William T Tran<sup>136</sup>, Jeroen van der Laak<sup>37</sup>, Gregory E Verghese<sup>54,55</sup>, Giuseppe Viale<sup>137</sup>, Noorul Wahab<sup>138</sup>, Thomas Walter<sup>81,82,83</sup>, Yannick Waumans<sup>139</sup>, Hannah Y Wen<sup>57</sup>, Wentao Yang<sup>140</sup>, Yinyin Yuan<sup>141</sup>, John Bartlett<sup>142</sup>, Sibylle Loibl<sup>143</sup>, Carsten Denkert<sup>144</sup>, Peter Savas<sup>145,146</sup>, Sherene Loi<sup>145,147</sup>, Elisabeth Specht Stovgaard<sup>148</sup>, Roberto Salgado<sup>3,145</sup>, William M Gallagher<sup>1</sup>, Arman Rahman<sup>149,\*</sup>

## Affiliations

- <sup>1</sup>UCD School of Biomolecular and Biomedical Science, UCD Conway Institute, University College Dublin, Dublin, Ireland
- <sup>2</sup>Earle A Chiles Research Institute, Providence Cancer Institute, Portland, OR, USA
- <sup>3</sup>Department of Pathology PA<sup>2</sup>, GZA-ZNA Hospitals, Antwerp, Belgium
- <sup>4</sup>Centre for Oncological Research (CORE), MIPPRO, Faculty of Medicine, Antwerp University, Antwerp, Belgium
- <sup>5</sup>Department of Pathology and Laboratory Medicine, Memorial Sloan Kettering Cancer Center, New York, NY, USA
- <sup>6</sup>Department of Pathology, Massachusetts General Hospital, Boston, MA, USA
- <sup>7</sup>Departments of Pathology and Dermatology, University of Michigan, Ann Arbor, MI, USA
- <sup>8</sup>Department of Biomedical informatics, Stony Brook University, Stony Brook, NY, USA
- <sup>9</sup>Institute of Pathology, Klinikum Bayreuth GmbH, Friedrich-Alexander-University Erlangen-Nuremberg, Bayreuth, Germany
- <sup>10</sup>Department of Pathology, Matsuyama Shimin Hospital, Matsuyama, Japan
- <sup>11</sup>Department of Pathology, Yale School of Medicine, New Haven, CT, USA
- <sup>12</sup>Department of Pathology and Laboratory Medicine, University of British Columbia, BC Cancer, Vancouver, British Columbia, Canada
- <sup>13</sup>Department of Pathology, University Medical Center Utrecht, Utrecht, The Netherlands
- <sup>14</sup>Johns Hopkins Oncology Center, Baltimore, MD, USA
- <sup>15</sup>Digestive Oncology, Department of Oncology, KU Leuven, Leuven, Belgium
- <sup>16</sup>Technical University of Denmark, Kgs. Lyngby, Denmark
- <sup>17</sup>Visiopharm A/S, Hørsholm, Denmark
- <sup>18</sup>Department of Cellular Pathology, University College Hospital, London, UK
- <sup>19</sup>Centre for Evolution and Cancer, The Institute of Cancer Research, London, UK
- <sup>20</sup>Hospital Maria Curie, Buenos Aires, Argentina
- <sup>21</sup>Department of Oncology and Pathology, Karolinska Institutet, Stockholm, Sweden
- <sup>22</sup>Department of Clinical Pathology and Cancer Diagnostics, Karolinska University Hospital, Stockholm, Sweden
- <sup>23</sup>Perlmutter Cancer Center, NYU Langone Health, New York, NY, USA



- <sup>24</sup>Department of Medicine, NYU Grossman School of Medicine, Manhattan, NY, USA
- <sup>25</sup>Division of Cancer Epidemiology and Genetics (DCEG), National Cancer Institute (NCI), Rockville, MD, USA
- <sup>26</sup>Oncology Hospital, Star Medica Centro, Juarez City, Mexico
- <sup>27</sup>Tehran University of Medical Sciences, Tehran, Iran
- <sup>28</sup>Department of Pathology and Laboratory Medicine, Emory University School of Medicine, Emory University Winship Cancer Institute, Atlanta, GA, USA
- <sup>29</sup>The National University of Malaysia, Kuala Lumpur, Malaysia
- <sup>30</sup>Departamento de Anatomía Patológica, Facultad de Medicina, Universidad de La Frontera, Temuco, Chile
- <sup>31</sup>Department of Pathology, Narayana Medical College, Nellore, India
- <sup>32</sup>Department of internal Medicine Section of Medical Oncology and Yale Cancer Center, Yale School of Medicine, New Haven, CT, USA
- <sup>33</sup>Department of Computer Science, Yale School of Engineering and Applied Science, New Haven, CT, USA
- <sup>34</sup>Amazonas Federal University, Manaus, Brazil
- <sup>35</sup>Pathology Department, Hospital Clínico Universitario de Valencia/Incliva, Valencia, Spain
- <sup>36</sup>Department of Pathobiology & Population Sciences, The Royal Veterinary College, London, UK
- <sup>37</sup>Head of Integrative Genomics Analysis in Clinical Trials, ICR-CTSU, Division of Clinical Studies, The Institute of Cancer Research, London, UK
- <sup>38</sup>Department of Pathology, Radboud University Medical Center, Nijmegen, The Netherlands
- <sup>39</sup>Department of Pathology, Northwestern Feinberg School of Medicine, Chicago, IL, USA
- <sup>40</sup>Department of Oncology, Laboratory of Tumor Immunology and Immunotherapy, KU Leuven, Leuven, Belgium
- <sup>41</sup>Biomedical Engineering Department, Emory University, Atlanta, GA, USA
- <sup>42</sup>Hospital Universitário Getúlio Vargas, Manaus, Brazil
- <sup>43</sup>Department of Radiation Oncology, Weill Cornell Medical College, New York, NY, USA
- <sup>44</sup>Department of Pathology, Weill Cornell Medicine, New York NY, USA
- <sup>45</sup>Computational Biology and Bioinformatics, Yale University, New Haven, CT, USA
- <sup>46</sup>University of Surrey, Guildford, UK

- <sup>47</sup>Ain Shams University, Cairo, Egypt
- <sup>48</sup>Institute Universitario de Investigación en Tecnología Centrada en el Ser Humano, HUMAN-tech, Universitat Politècnica de València, Valencia, Spain
- <sup>49</sup>Montefiore Medical Center and the Albert Einstein College of Medicine, New York, NY, USA
- <sup>50</sup>Pathology, Peter MacCallum Cancer Centre and Sir Peter MacCallum Department of Oncology, University of Melbourne, Melbourne, Victoria, Australia
- <sup>51</sup>Genentech, San Francisco, CA, USA
- <sup>52</sup>Department of Oncological Sciences, Medicine Hem/One, and Pathology, Tisch Cancer Institute – Precision Immunology Institute, Icahn School of Medicine at Mount Sinai, New York NY, USA
- <sup>53</sup>Department of Medicine, Vanderbilt University Medical Center, Nashville, TN, USA
- <sup>54</sup>Cancer Bioinformatics, Faculty of Life Sciences and Medicine, School of Cancer & Pharmaceutical Sciences, King's College London, London, UK
- <sup>55</sup>The Breast Cancer Now Research Unit Faculty of Life Sciences and Medicine, School of Cancer and Pharmaceutical Sciences, King's College London, London, UK
- <sup>56</sup>Department of Translational Immunotherapy, German Cancer Research Center, Heidelberg, Germany
- <sup>57</sup>Memorial Sloan Kettering Cancer Center, New York, NY, USA
- <sup>58</sup>Case Western University, Cleveland, OH, USA
- <sup>59</sup>Department of Laboratory Medicine and Pathology, Mayo Clinic, Rochester, MN, USA
- <sup>60</sup>Department of Oncology-Pathology, Karolinska Institutet, Stockholm, Sweden
- <sup>61</sup>Laboratory of Pathology, Center for Cancer Research, National Cancer Institute, National Institutes of Health, Bethesda, MD, USA
- <sup>62</sup>Division of Pathology, Netherlands Cancer Institute (NKI), Amsterdam, The Netherlands
- <sup>63</sup>Praava Health, Dhaka, Bangladesh
- <sup>64</sup>King's College London & Guys & St Thomas NHS Trust London, UK
- <sup>65</sup>Department of Pathology, Stavanger University Hospital, Stavanger, Norway
- <sup>66</sup>Department of Chemistry, Bioscience and Environmental Technology, University of Stavanger, Stavanger, Norway
- <sup>67</sup>Department of Pathology, Iwate Medical University, Morioka, Japan
- <sup>68</sup>Department of Breast Surgery, Kyoto University Graduate School of Medicine, Kyoto, Japan

- <sup>69</sup>Department of Pathology and Laboratory Medicine, Ann & Robert H. Lurie Children's Hospital of Chicago, Chicago, IL, USA
- <sup>70</sup>Histopathology, Aakash Healthcare Super Speciality Hospital, New Delhi, India
- <sup>71</sup>Department of Pathology, Netherlands Cancer Institute – Antoni van Leeuwenhoek Hospital, Amsterdam, The Netherlands
- <sup>72</sup>Data, Analytics and Imaging, Product Development, F. Hoffmann-La Roche AG, Basel, Switzerland
- <sup>73</sup>Translational Molecular Biomarkers, Merck & Co., Inc., Kenilworth, NJ, USA
- <sup>74</sup>Translational Medicine, Bristol Myers Squibb, Princeton, NJ, USA
- <sup>75</sup>Department of Clinical Pathology, Sahlgrenska University Hospital, Gothenburg, Sweden
- <sup>76</sup>Institute of Biomedicine, Sahlgrenska Academy, University of Gothenburg, Gothenburg, Sweden
- <sup>77</sup>Department of Surgical Pathology, Zealand University Hospital, Roskilde, Denmark
- <sup>78</sup>Department of Surgical Pathology, University of Copenhagen, Copenhagen, Denmark
- <sup>79</sup>Institut Jules Bordet Université Libre de Bruxelles, Brussels, Belgium
- <sup>80</sup>Center for Integrated Diagnostics, Massachusetts General Hospital/Harvard Medical School, Boston, MA, USA
- <sup>81</sup>Centre for Computational Biology (CBIO), Mines Paris, PSL University, Paris, France
- <sup>82</sup>Institut Curie, PSL University, Paris, France
- <sup>83</sup>INSERM U900, Paris, France
- <sup>84</sup>Department of Pathology and Laboratory Medicine, Emory University, Atlanta, GA, USA
- <sup>85</sup>Department of Biomedical Engineering, Radiology and Imaging Sciences, Biomedical Informatics, Pathology, Georgia Institute of Technology and Emory University, Atlanta, GA, USA
- <sup>86</sup>NRG Oncology/NSABP Foundation, Pittsburgh, PA, USA
- <sup>87</sup>Manipal Hospitals, Bangalore, India
- <sup>88</sup>Breast Cancer Translational Research Group, University of Pennsylvania, Philadelphia, PA, USA
- <sup>89</sup>Indian Cancer Genomic Atlas, Pune, India
- <sup>90</sup>Centre for Health, Innovation and Policy Foundation, Noida, India

- <sup>91</sup>Office of Biostatistics and Epidemiology, Gustave Roussy, Oncostat U1018, Inserm, University Paris-Saclay, Ligue Contre le Cancer labeled Team, Villejuif France
- <sup>92</sup>Department of Pathology, Narayana Medical College and Hospital, Nellore, India
- <sup>93</sup>Tissue Image Analytics Centre, Warwick Cancer Research Centre, PathLAKE Consortium, Department of Computer Science, University of Warwick, Coventry, UK
- <sup>94</sup>Department of Chemical Engineering, Department of Laboratory Medicine and Pathology, University of Washington, Seattle, Washington, USA
- <sup>95</sup>CRUK Lung Cancer Centre of Excellence, UCL and Cellular Pathology Department UCLH, London, UK
- <sup>96</sup>Department of Biochemistry, Ziauddin University, Karachi, Pakistan
- <sup>97</sup>Pathology and Laboratory Medicine, All India Institute of Medical Sciences, Raipur, India
- <sup>98</sup>Institute of Metabolism and Systems Research, University of Birmingham, Birmingham, UK
- <sup>99</sup>Department of Clinical Pathology, Drammen Sykehus, Vestre Viken HF, Drammen, Norway
- <sup>100</sup>Service de Pathologie et Biopathologie, Centre Jean PERRIN, INSERM U1240 Imagerie Moléculaire et Stratégies Théranostiques (IMoST), Université Clermont Auvergne, Clermont-Ferrand, France
- <sup>101</sup>School of Electrical, Mechanical and Infrastructure Engineering, University of Melbourne, Melbourne, Victoria, Australia
- <sup>102</sup>Division of Cancer Research, Peter MacCallum Cancer Centre, Melbourne, Victoria, Australia
- <sup>103</sup>Radiogenomics Laboratory, Sunnybrook Health Sciences Centre, Toronto, Ontario, Canada
- <sup>104</sup>Department of Clinical Studies, Ontario Veterinary College, University of Guelph, Guelph, Ontario, Canada
- <sup>105</sup>Department of Oncology, Lakeshore Animal Health Partners, Mississauga, Ontario, Canada
- <sup>106</sup>Centre for Advancing Responsible and Ethical Artificial Intelligence (CARE-AI), University of Guelph, Guelph, Ontario, Canada
- <sup>107</sup>Diagnostico de Salud Animal SA, Ciudad de México, Mexico
- <sup>108</sup>Department of Pathology and Laboratory Medicine, Fondazione IRCCS Istituto Nazionale dei Tumori, Milan, Italy
- <sup>109</sup>Faculty of Medicine and Surgery, University of Milan, Milan, Italy
- <sup>110</sup>Yale Cancer Center, Yale University, New Haven, CT, USA

- <sup>111</sup>Department of Medical Oncology, Yale School of Medicine, Yale University, New Haven, CT, USA
- <sup>112</sup>University of Warwick Coventry, UK
- <sup>113</sup>The Medical Oncology Centre of Rosebank Johannesburg South Africa
- <sup>114</sup>Department of Immunology, Faculty of Health Sciences, University of Pretoria, Pretoria, South Africa
- <sup>115</sup>Institute of Pathology, University Hospital Düsseldorf and Heinrich-Heine-University, Düsseldorf Germany
- <sup>116</sup>Breast Unit Institute Gustave Roussy, Villejuif France
- <sup>117</sup>Department of Pathology, Yale University School of Medicine, New Haven, CT, USA
- <sup>118</sup>Department of Medicine, Yale University School of Medicine, New Haven, CT, USA
- <sup>119</sup>Department of Diagnostic and Theranostic Medicine, Institut Curie, University Paris-Sciences et Lettres, Paris, France
- <sup>120</sup>Department of Biomedical Informatics, Stony Brook Medicine, New York NY, USA
- <sup>121</sup>Department of Pathology, Aga Khan University, Nairobi, Kenya
- <sup>122</sup>iRhythm Technologies Inc., San Francisco, CA, USA
- <sup>123</sup>Mater Misericordiae University Hospital, Dublin, Ireland
- <sup>124</sup>Department of Pathology, Section of Breast Pathology, Northwestern University Feinberg School of Medicine, Chicago, IL, USA
- <sup>125</sup>Breast Cancer Translational Research Laboratory J.-C. Heuson, Institut Jules Bordet Hôpital Universitaire de Bruxelles (H.U.B), Université Libre de Bruxelles (ULB), Brussels, Belgium
- <sup>126</sup>Medical Oncology Department Institut Jules Bordet Hôpital Universitaire de Bruxelles (H.U.B), Université Libre de Bruxelles (ULB), Brussels, Belgium
- <sup>127</sup>Institute of Pathology, University Hospital Heidelberg, Centers for Personalized Medicine (ZPM), Heidelberg, Germany
- <sup>128</sup>King Hussein Cancer Center, Amman, Jordan
- <sup>129</sup>Department of Medical Oncology, University of Medicine and Pharmacy "Iuliu Hatieganu ", Cluj-Napoca, Romania
- <sup>130</sup>University of Texas MD Anderson Cancer Center, Houston, TX, USA
- <sup>131</sup>Kyoto University, Kyoto, Japan
- <sup>132</sup>Tempus Labs, Chicago, IL, USA
- <sup>133</sup>AI for Oncology Lab, The Netherlands Cancer Institute, Amsterdam, The Netherlands

- <sup>134</sup>Mayo Clinic, Jacksonville, FL, USA
- <sup>135</sup>Department of Pathology, Institute of Clinical Medicine, Aarhus University Hospital, Aarhus, Denmark
- <sup>136</sup>Department of Radiation Oncology, University of Toronto and Sunnybrook Health Sciences Centre, Toronto, Canada
- <sup>137</sup>Department of Pathology, European Institute of Oncology & University of Milan, Milan, Italy
- <sup>138</sup>Tissue Image Analytics Centre, Department of Computer Science, University of Warwick Coventry, UK
- <sup>139</sup>CellCarta NV, Antwerp, Belgium
- <sup>140</sup>Fudan Medical University Shanghai Cancer Center, Shanghai, PR China
- <sup>141</sup>Department of Translational Molecular Pathology, Division of Pathology and Laboratory Medicine, The University of Texas MD Anderson Cancer Center, Houston, TX, USA
- <sup>142</sup>University of Edinburgh, Edinburgh, UK
- <sup>143</sup>Department of Medicine and Research, German Breast Group, Neu-Isenburg Germany
- <sup>144</sup>Institut für Pathologie, Philipps-Universität Marburg und Universitätsklinikum Marburg, Marburg, Germany
- <sup>145</sup>Division of Cancer Research, Peter MacCallum Cancer Centre, Melbourne, Victoria, Australia
- <sup>146</sup>The Sir Peter MacCallum Department of Medical Oncology, University of Melbourne, Melbourne, Victoria, Australia
- <sup>147</sup>Sir Peter MacCallum Department of Oncology, The University of Melbourne, Melbourne, Victoria, Australia
- <sup>148</sup>Department of Pathology, Herlev and Gentofte Hospital, Herlev, Denmark
- <sup>149</sup>UCD School of Medicine, UCD Conway Institute, University College Dublin, Dublin, Ireland

## Acknowledgements

GB was funded by the Gilead Breast Cancer Research Grant 2023. JSR-F was funded in part by the Breast Cancer Research Foundation, a Susan G Komen Leadership Grant, and NIH/NCI P50 CA247749 01 grant. SV was supported by Interne Fondsen KU Leuven/Internal Funds KU Leuven. BA received the Swedish Society for Medical Research (Svenska Sällskapet för Medicinsk Forskning) Postdoctoral Grant and the Swedish Breast Cancer Association (Bröstcancerförbundet) Research Grant 2021. GC was supported by the Peer Reviewed Cancer Research Program (Award W81XWH-21-1-0160) from the US Department of Defense and the Mayo Clinic Breast Cancer SPORE Grant P50 CA116201 from the NIH. CF-M was funded by the Horizon 2020 European Union research and innovation programme under the Marie Skłodowska Curie grant agreement no. 860627 (CLARIFY Project). SBF: NHMRC GNT1193630. SG was partially supported by NIH Grant CA224319, DK124165, CA263705, and CA196521. AG was supported by Breast Cancer Now (and their legacy charity Breakthrough Breast Cancer) and Cancer Research UK (CRUK/07/012, KCL-BCN-Q3). TRK: Japan Society for the Promotion of Science (JSPS) KAKENHI (21K06909). UK



was funded by the Horizon 2020 European Union Research and Innovation Programme under the Marie Skłodowska-Curie grant agreement no. 860627 (CLARIFY Project). JKL was in part supported by National Institutes of Health (NIH) (R37CA225655). AM was supported by the National Cancer Institute under award numbers R01CA268287A1, U01CA269181, R01CA26820701A1, R01CA249992-01A1, R01CA202752-01A1, R01CA208236-01A1, R01CA216579-01A1, R01CA220581-01A1, R01CA257612-01A1, 1U01CA239055-01, 1U01CA248226-01, 1U54CA254566-01, National Heart, Lung and Blood Institute 1R01HL15127701A1, R01HL15807101A1, National Institute of Biomedical Imaging and Bioengineering 1R43EB028736-01, VA Merit Review Award IBX004121A from the US Department of Veterans Affairs Biomedical Laboratory Research and Development Service the Office of the Assistant Secretary of Defense for Health Affairs, through the Breast Cancer Research Program (W81XWH-19-1-0668), the Prostate Cancer Research Program (W81XWH-20-1-0851), the Lung Cancer Research Program (W81XWH-18-1-0440, W81XWH-20-1-0595), the Peer Reviewed Cancer Research Program (W81XWH-18-1-0404, W81XWH-21-1-0345, W81XWH-21-1-0160), the Kidney Precision Medicine Project (KPMP) Glue Grant and sponsored research agreements from Bristol Myers Squibb, Boehringer-Ingelheim, Eli Lilly and AstraZeneca. SKM thanks Kay Pogue-Geile, Director of Molecular Profiling at NSABP for her constant support and encouragement, Roberto Salgado, for getting me initiated into the wonderful subject of immuno-oncology and its possibilities. FuAM received funding from EPSRC EP/W02909X/1 and PathLAKE consortium. FP-L received research grants from Fondation ARC, La Ligue contre le Cancer. RDP received the Melbourne Research Scholarship and a scholarship from the Peter MacCallum Cancer Centre. JS: UH3CA225021, U24CA215109. ST was supported by Interne Fondsen KU Leuven/Internal Funds KU Leuven. JT was supported by institutional grants of the KWF Kankerbestrijding and the Dutch Ministry of Health, Welfare and Sport. EAT received the Breast Cancer Research Foundation Grant 22-161. GEV was supported by Breast Cancer Now (and their legacy charity Breakthrough Breast Cancer) and Cancer Research UK (CRUK/07/012, KCL-BCN-Q3). TW was supported by the French Government under management of Agence Nationale de la Recherche as part of the 'Investissements d'avenir' program, reference ANR-19-P3IA-0001 (PRAIRIE 3IA Institute) and by Q-Life (ANR-17-CONV-0005). HYW was funded in part by the NIH/NCI P50 CA247749 01 grant. YY received funding from Cancer Research UK Career Establishment Award (CRUK C45982/A21808). PS received funding support from the National Health and Medical Research Council, Australia. SL was supported by the National Breast Cancer Foundation of Australia (NBCF) (APP ID: EC-17-001), the Breast Cancer Research Foundation, New York (BCRF (APP ID: BCRF-21-102), and a National Health and Medical Council of Australia (NHMRC) Investigator Grant (APP ID: 1162318). RS was supported by the Breast Cancer Research Foundation (BCRF, grant no. 17-194). WMG was supported by the North-South Research Programme administered by the Higher Education Authority on behalf of the Department of Further and Higher Education, Research, Innovation and Science and the Shared Island Fund (AICRIstart: A Foundation Stone for the All-Island Cancer Research Institute (AICRI): Building Critical Mass in Precision Cancer Medicine <https://www.aicri.org/aicristart>), Irish Cancer Society (Collaborative Cancer Research Centre BREAST-PREDICT; CCRC13GAL; <https://www.breastpredict.com>), the Science Foundation Ireland Investigator Programme (OPTI-PREDICT; 15/IA/3104), the Science Foundation Ireland Strategic Partnership Programme (Precision Oncology Ireland; 18/SPP/3522; <https://www.precisiononcology.ie>). Open access funding provided by IReL.

#### Conflict of interest statement:

DBP: Speaker's Bureau: Genentech, Novartis, Clinical Care Options, Oncocyte; research support: WindMIL, Brooklyn Immunotherapeutics, Merck, Bristol Myers Squibb, IMV; consulting: Merck, Biotheranostics, Puma, Gilead, Lilly, Sanofi, NGM Bio, Sanford Burnham Prebys, AstraZeneca. GB: Speaker's fee from MSD and Novartis, advisory boards for Roche and MSD, consultant for MSD, Novartis, and Roche, travel and conference support from Roche, MSD, and Gilead. JSR-F is an Associate Editor of The Journal of Pathology and has received personal/consultancy fees from Goldman Sachs, Bain Capital, REPARE Therapeutics, Saga Diagnostics, and PaigeAI, membership of the scientific advisory boards of VolitionRx, REPARE Therapeutics, and Paige. AI, membership of the Board of Directors of Grupo Oncoclinicas, and ad hoc membership of the scientific advisory boards of AstraZeneca, Merck Daiichi Sankyo, Roche Tissue Diagnostics, and Personalis, outside the scope of this study. AIH: Research fund from Visiopharm A/S. ZK: Paid advisory role for Eli Lilly and AstraZeneca Canada. JT: Employee of Visiopharm A/S. KRMB: Scientific Advisory Board for CDI Labs, research funding form Carevive. FC: Chair of the Scientific and Medical Advisory Board of TRIBVN Healthcare, France, and advisory board fees from TRIBVN Healthcare, France in the last 5 years. Shareholder of Aiosyn BV, the Netherlands. LADC: Participation in the Tempus Algorithm Advisors program. AC: Contracted researcher for Oncoinvent AS and Novocure and a consultant for Sotio a.s. and Epics Therapeutics SA. ME: Egyptian missions sector. SBF: Expert advisory panel for AXDEV Group. JMG: Employee and stockholder of Roche/Genentech. SG: Research funding from Regeneron Pharmaceuticals, Boehringer Ingelheim, Bristol Myers Squibb, Celgene, Genentech, EMD Serono, Pfizer, and Takeda, unrelated to the current work; named co-inventor on an issued patent for multiplex immunohistochemistry to characterise tumours and treatment responses. The technology is filed through Icahn School of Medicine at Mount Sinai (ISMMS) and is currently unlicensed. NH: Patent on a technology to measure immune infiltration in cancer to predict treatment outcome (W02012038068A2). MGH: Consultant for PaigeAI, VolastraTx, and advisor for PathPresenter. JH: Speaker's honoraria or advisory board remunerations from Roche, Novartis, AstraZeneca, Eli Lilly, and MSD. Co-founder and shareholder of Stratipath AB. KK Employee and stockholder of Roche. GA: Employee of Merck & Co Inc. AIK: Honorarium from Roche, MSD, and Pfizer, member of the Advisory Board of Pfizer. A-VL Institutional grants from AstraZeneca and personal grants from

AstraZeneca (travel and honorarium from advisory board), MSD (honorarium from advisory board), and Daiichi Sankyo (travel). XL: Eli Lilly Company, Advisor, Cancer Expert Now, Advisor, Champions Oncology, Research fund. AM: Equity holder in Picture Health, Elucid Bioimaging and Inspirata Inc, advisory board of Picture Health, Aiforia Inc and SimBioSys, consultant for SimBioSys, sponsored research agreements with AstraZeneca, Boehringer-Ingelheim, Eli-Lilly, and Bristol Myers Squibb, technology licensed to Picture Health and Elucid Bioimaging involvement in three different R01 grants with Inspirata Inc DKM: Consulting: Astrazeneca, Lilly USA LLC Hologic. Sponsored Research: Merck Agendia. SM: Scientific Committee Study member. Roche, data and safety monitoring member of clinical trials: Sensorion, Biophytis, Servier, IQVIA, Yuhan, Kedrion. FuAAM: Research studentship funding from GSK DAM: Speaker fees from AstraZeneca, Eli Lilly, and Takeda, consultancy fees from AstraZeneca, Thermo Fisher, Takeda, Amgen, Janssen, M/M Software, Bristol Myers Squibb, and Eli Lilly, educational support from Takeda and Amgen. FP-L: Personal financial interests: AbbVie, Agendia, Amgen, Astellas, AstraZeneca, Bayer, BMS, Daiichi-Sankyo, Eisai, Exact Science, GSK Illumina, Incyte, Janssen, Lilly, MERCK lifa, Merck-MSD, Myriad, Novartis, Pfizer, Pierre-Fabre, Roche, Sanofi, Seagen, Takeda, VeracYTE, Servier. Institutional financial interests: AstraZeneca, Bayer, BMS, MSD, Myriad, Roche, VeracYTE. Congress invitations: AbbVie, Amgen, AstraZeneca, Bayer, BMS, Gilead, MSD, Novartis, Roche, Lilly, Pfizer. NMR: Co-Founder, Director and CSO of Histofy Ltd, UK AS: Advisory Board/Speaker's Bureau: Aignostics, AstraZeneca, Bayer, BMS, Eli Lilly, Illumina, Incyte, Janssen, MSD, Novartis, Pfizer, Roche, Seagen, Takeda, and Thermo Fisher; grants from Bayer, Bristol Meyers Squibb, Chugai, and Incyte. TT: Employee of Tempus Labs. JT: Shareholder of EllogonAI BV. TT: Speaker's fee from Pfizer. JvdL: Member of the advisory boards of Philips, the Netherlands and ContextVision, Sweden, research funding from Philips, the Netherlands, ContextVision, Sweden, and Sectra, Sweden in the last 5 years. Chief scientific officer and shareholder of Aiosyn BV, the Netherlands. TW: Collaboration with TRIBUN Health on automatic grading of biopsies for head and neck cancer, patent on the prediction of homologous recombination deficiency in breast cancer. YW: Employee of CellCarta. HYW: Advisory faculty of AstraZeneca. YY: Speaker/consultant for Roche and Merck PS: Consultant (uncompensated) to Roche-Genentech. SL Research funding to institution from Novartis, Bristol Meyers Squibb, Merck Puma Biotechnology, Eli Lilly, Nektar Therapeutics, AstraZeneca, Roche-Genentech, and Seattle Genetics. Consultant (not compensated) to Seattle Genetics, Novartis, Bristol Meyers Squibb, Merck, AstraZeneca, Eli Lilly, Pfizer, and Roche-Genentech. Consultant (paid to her institution) to Aduro Biotech, Novartis, GlaxoSmithKline, Roche-Genentech, AstraZeneca, Silverback Therapeutics, GI Therapeutics, PUMA Biotechnologies, Pfizer, Gilead Therapeutics, Seattle Genetics, Daiichi-Sankyo, Amunix, Tallac therapeutics, Eli Lilly, and Bristol Meyers Squibb. RS: Non-financial support from Merck and Bristol Myers Squibb, research support from Merck Puma Biotechnology and Roche; personal fees from Roche, Bristol Myers Squibb and Exact Sciences for advisory boards. WMG: Co-founder, shareholder and part-time Chief Scientific Officer of OncoAssure Limited, shareholder in Deciphex and member of the Scientific Advisory Board of Carrick Therapeutics.

## References

- Hanahan D, Weinberg RA. Hallmarks of cancer: the next generation. *Cell* 2011; 144: 646–674. [PubMed: 21376230]
- Chen DS, Mellman I. Oncology meets immunology: the cancer-immunity cycle. *Immunity* 2013; 39: 1–10. [PubMed: 23890059]
- Gonzalez H, Hagerling C, Werb Z. Roles of the immune system in cancer: from tumor initiation to metastatic progression. *Genes Dev* 2018; 32: 1267–1284. [PubMed: 30275043]
- Zamarron BF, Chen W. Dual roles of immune cells and their factors in cancer development and progression. *Int J Biol Sci* 2011; 7:651–658. [PubMed: 21647333]
- Ribatti D The concept of immune surveillance against tumors. The first theories. *Oncotarget* 2017; 8: 7175–7180. [PubMed: 27764780]
- Fridman WH, Zitvogel L, Sautès-Fridman C, et al. The immune contexture in cancer prognosis and treatment. *Nat Rev Clin Oncol* 2017; 14: 717–734. [PubMed: 28741618]
- Barnes TA, Amir E. HYPE or HOPE: the prognostic value of infiltrating immune cells in cancer. *Br J Cancer* 2017; 117:451–60. [PubMed: 28704840]
- Chen B, Li H, Liu C, et al. Prognostic value of the common tumour-infiltrating lymphocyte subtypes for patients with non-small cell lung cancer: a meta-analysis. *PLoS One* 2020; 15: e0242173. [PubMed: 33170901]
- Fu Q, Chen N, Ge C, et al. Prognostic value of tumor-infiltrating lymphocytes in melanoma: a systematic review and meta-analysis. *Oncoimmunology* 2019; 8: e1593806.
- Galon J, Costes A, Sanchez-Cabo F, et al. Type, density, and location of immune cells within human colorectal tumors predict clinical outcome. *Science* 2006; 313: 1960–1964. [PubMed: 17008531]

11. Schulze AB, Evers G, Görlich D, et al. Tumor infiltrating T cells influence prognosis in stage I–III non-small cell lung cancer. *J Thorac Dis* 2020; 12: 1824–1842. [PubMed: 32642087]
12. Wells DK, Chuang Y, Knapp LM, et al. Spatial and functional heterogeneities shape collective behavior of tumor-immune networks. *PLoS Comput Biol* 2015; 11: e 1004181.
13. Tan WCC, Nerurkar SN, Cai HY, et al. Overview of multiplex immunohistochemistry/immunofluorescence techniques in the era of cancer immunotherapy. *Cancer Commun* 2020; 40: 135–153.
14. Ventola CL. Cancer immunotherapy, part 3: challenges and future trends. *P T* 2017; 42: 514–521. [PubMed: 28781505]
15. Lu S, Stein JE, Rimm DL, et al. Comparison of biomarker modalities for predicting response to PD-1/PD-L1 checkpoint blockade: a systematic review and meta-analysis. *JAMA Oncol* 2019; 5: 1195–1204. [PubMed: 31318407]
16. Chan RCK, Li JJX, Yeung W, et al. Virtual multiplex immunohistochemistry: application on cell block of effusion and aspiration cytology. *Diagn Cytopathol* 2020; 48: 417–423. [PubMed: 32017459]
17. Locke D, Hoyt CC. Companion diagnostic requirements for spatial biology using multiplex immunofluorescence and multispectral imaging. *Front Mol Biosci* 2023; 10: 1051491.
18. Hendry S, Salgado R, Gevaert T, et al. Assessing tumor-infiltrating lymphocytes in solid tumors: a practical review for pathologists and proposal for a standardized method from the international Immunooncology biomarkers working group: part 1: assessing the host immune response, TILs in invasive breast carcinoma and ductal carcinoma in situ, metastatic tumor deposits and areas for further research. *Adv Anat Pathol* 2017; 24: 235–251. [PubMed: 28777142]
19. Salgado R, Denkert C, Demaria S, et al. The evaluation of tumor-infiltrating lymphocytes (TILs) in breast cancer: recommendations by an international TILs working group 2014. *Ann Oncol* 2015; 26: 259–271. [PubMed: 25214542]
20. Halse H, Colebatch AJ, Petrone P, et al. Multiplex immunohistochemistry accurately defines the immune context of metastatic melanoma. *Sci Rep* 2018; 8: 11158.
21. Mori H, Bolen J, Schuetter L, et al. Characterizing the tumor immune microenvironment with tyramide-based multiplex immunofluorescence. *J Mammary Gland Biol Neoplasia* 2020; 25: 417–432. [PubMed: 33590360]
22. Lee SL, Cabanero M, Hyrcza M, et al. Computer-assisted image analysis of the tumor microenvironment on an oral tongue squamous cell carcinoma tissue microarray. *Clin Transl Radiat Oncol* 2019; 17: 32–39. [PubMed: 31193592]
23. Schüffler PJ, Schapiro D, Giesen C, et al. Automatic single cell segmentation on highly multiplexed tissue images. *Cytometry A* 2015; 87: 936–942. [PubMed: 26147066]
24. Hoyt CC. Multiplex immunofluorescence and multispectral imaging: forming the basis of a clinical test platform for Immuno-oncology. *Front Mol Biosci* 2021; 8: 674747.
25. Abousamra S, Gupta R, Hou L, et al. Deep learning-based mapping of tumor infiltrating lymphocytes in whole slide images of 23 types of cancer. *Front Oncol* 2022; 11: 806603.
26. Lu Z, Xu S, Shao W, et al. Deep-learning-based characterization of tumor-infiltrating lymphocytes in breast cancers from histopathology images and multiomics data. *JCO Clin Cancer Inform* 2020; 4: 480–490. [PubMed: 32453636]
27. Bulten W, Bándi P, Hoven J, et al. Epithelium segmentation using deep learning in H&E-stained prostate specimens with immunohistochemistry as reference standard. *Sci Rep* 2019; 9: 864. [PubMed: 30696866]
28. Nagpal K, Foote D, Liu Y, et al. Development and validation of a deep learning algorithm for improving Gleason scoring of prostate cancer. *NPJ Digit Med* 2019; 2: 48. [PubMed: 31304394]
29. Ehteshami Bejnordi B, Veta M, van Diest PJ, et al. Diagnostic assessment of deep learning algorithms for detection of lymph node metastases in women with breast cancer. *JAMA* 2017; 318: 2199–2210. [PubMed: 29234806]
30. Vance K, Alitinok A, Winfree S, et al. Machine learning analyses of highly-multiplexed immunofluorescence identifies distinct tumor and stromal cell populations in primary pancreatic tumors. *Cancer Biomark* 2022; 33: 219–235. [PubMed: 35213363]

31. Zarubin D, Belotskiy V, Xiang Z, et al. A clinical AI-driven multiplex immunofluorescence imaging pipeline to characterize tumor microenvironment heterogeneity. *J Clin Oncol* 2022; 40: 3020. [PubMed: 35436146]
32. Fassler DJ, Abousamra S, Gupta R, et al. Deep learning-based image analysis methods for brightfield-acquired multiplex immunohistochemistry images. *Diagn Pathol* 2020; 15: 100. [PubMed: 32723384]
33. Parra ER. Methods to determine and analyze the cellular spatial distribution extracted from multiplex immunofluorescence data to understand the tumor microenvironment. *Front Mol Biosci* 2021; 8: 668340.
34. Rojas F, Hernandez S, Lazcano R, et al. Multiplex immunofluorescence and the digital image analysis workflow for evaluation of the tumor immune environment in translational research. *Front Oncol* 2022; 12: 889886.
35. Viratham Pulsawatdi A, Craig SG, Bingham V, et al. A robust multiplex immunofluorescence and digital pathology workflow for the characterisation of the tumour immune microenvironment. *Mol Oncol* 2020; 14: 2384–2402. [PubMed: 32671911]
36. Parra ER, Jiang M, Solis L, et al. Procedural requirements and recommendations for multiplex immunofluorescence tyramide signal amplification assays to support translational oncology studies. *Cancers (Basel)* 2020; 12: 255. [PubMed: 31972974]
37. Taube JM, Akturk G, Angelo M, et al. The Society for Immunotherapy of cancer statement on best practices for multiplex immunohistochemistry (IHC) and immunofluorescence (IF) staining and validation. *J Immunother Cancer* 2020; 8: e000155. [PubMed: 32414858]
38. Khouja MH, Baekelandt M, Sarab A, et al. Limitations of tissue microarrays compared with whole tissue sections in survival analysis. *Oncol Lett* 2010; 1: 827–831. [PubMed: 22966388]
39. Obeid JM, Hu Y, Erdag G, et al. The heterogeneity of tumor-infiltrating CD8+ T cells in metastatic melanoma distorts their quantification: how to manage heterogeneity? *Melanoma Res* 2017; 27: 211–217. [PubMed: 28118270]
40. Nederlof I, De Bortoli D, Bareche Y, et al. Comprehensive evaluation of methods to assess overall and cell-specific immune infiltrates in breast cancer. *Breast Cancer Res* 2019; 21: 151. [PubMed: 31878981]
41. Hoos A, Cordon-Cardo C. Tissue microarray profiling of cancer specimens and cell lines: opportunities and limitations. *Lab Invest* 2001; 81: 1331–1338. [PubMed: 11598146]
42. Camp RL, Charette LA, Rimm DL. Validation of tissue microarray technology in breast carcinoma. *Lab Invest* 2000; 80: 1943–1949. [PubMed: 11140706]
43. Kos Z, Roblin E, Kim RS, et al. Pitfalls in assessing stromal tumor infiltrating lymphocytes (sTILs) in breast cancer. *NPJ Breast Cancer* 2020; 6: 17. [PubMed: 32411819]
44. Mani NL, Schalper KA, Hatzis C, et al. Quantitative assessment of the spatial heterogeneity of tumor-infiltrating lymphocytes in breast cancer. *Breast Cancer Res* 2016; 18: 78. [PubMed: 27473061]
45. Althobiti M, Aleskandarany MA, Joseph C, et al. Heterogeneity of tumour-infiltrating lymphocytes in breast cancer and its prognostic significance. *Histopathology* 2018; 73: 887–896. [PubMed: 29947077]
46. König L, Mairinger FD, Hoffmann O, et al. Dissimilar patterns of tumor-infiltrating immune cells at the invasive tumor front and tumor center are associated with response to neoadjuvant chemotherapy in primary breast cancer. *BMC Cancer* 2019; 19: 120. [PubMed: 30717704]
47. Steele KE, Tan TH, Korn R, et al. Measuring multiple parameters of CD8+ tumor-infiltrating lymphocytes in human cancers by image analysis. *J Immunother Cancer* 2018; 6: 20. [PubMed: 29510739]
48. Galon J, Pages F, Marincola FM, et al. The immune score as a new possible approach for the classification of cancer. *J Transl Med* 2012; 10: 1. [PubMed: 22214470]
49. Pagès F, Mlecnik B, Marliot F, et al. International validation of the consensus immunoscore for the classification of colon cancer: a prognostic and accuracy study. *Lancet* 2018; 391: 2128–2139. [PubMed: 29754777]

50. Sanchez K, Kim I, Chun B, et al. Multiplex immunofluorescence to measure dynamic changes in tumor-infiltrating lymphocytes and PD-L1 in early-stage breast cancer. *Breast Cancer Res* 2021; 23: 2. [PubMed: 33413574]
51. spatstat: Spatial Point Pattern Analysis, Model-Fitting, Simulation, Tests. Available from: <https://CRAN.R-project.org/package=spatstat>
52. Page DB, Broeckz G, Jahangir CA, et al. Spatial analyses of immune cell infiltration in cancer: current methods and future directions: a report of the International Immuno-oncology Biomarker Working Group on Breast Cancer. *J Pathol* 2023; 260: 514–532. [PubMed: 37608771]
53. Giraldo NA, Sanchez-Salas R, Peske JD, et al. The clinical role of the TME in solid cancer. *Br J Cancer* 2019; 120: 45–53. [PubMed: 30413828]
54. Galon J, Mlecnik B, Marliot F, et al. Validation of the immunoscore (IM) as a prognostic marker in stage I/II/III colon cancer: results of a worldwide consortium-based analysis of 1,336 patients. *J Clin Oncol* 2016; 34: 3500.
55. Angell HK, Bruni D, Barrett JC, et al. The immunoscore: colon cancer and beyond. *Clin Cancer Res* 2020; 26: 332–339. [PubMed: 31413009]
56. Galon J, Mlecnik B, Bindea G, et al. Towards the introduction of the ‘Immunoscore’ in the classification of malignant tumours. *J Pathol* 2014; 232: 199–209. [PubMed: 24122236]
57. Lyons YA, Wu SY, Overwijk WW, et al. Immune cell profiling in cancer: molecular approaches to cell-specific identification. *NPJ Precis Oncol* 2017; 1: 26. [PubMed: 29872708]
58. Bai R, Lv Z, Xu D, et al. Predictive biomarkers for cancer immunotherapy with immune checkpoint inhibitors. *Biomark Res* 2020; 8: 34. [PubMed: 32864131]
59. Waldman AD, Fritz JM, Lenardo MJ. A guide to cancer immunotherapy: from T cell basic science to clinical practice. *Nat Rev Immunol* 2020; 20: 651–668. [PubMed: 32433532]
60. Anandappa AJ, Wu CJ, Ott PA. Directing traffic: how to effectively drive T cells into tumors. *Cancer Discov* 2020; 10: 185–197. [PubMed: 31974169]
61. Ochoa De Olza M, Navarro Rodrigo B, Zimmermann S, et al. Turning up the heat on non-immunoreactive tumours: opportunities for clinical development. *Lancet Oncol* 2020; 21: e419–e430. [PubMed: 32888471]
62. Garaud S, Buisseret L, Solinas C, et al. Tumor infiltrating B-cells signal functional humoral immune responses in breast cancer. *JCI Insight* 2019; 4:e129641.
63. Egelston CA, Avalos C, Tu TY, et al. Resident memory CD8<sup>+</sup> T cells within cancer islands mediate survival in breast cancer patients. *JCI Insight* 2019; 4: e130000.
64. He T-F, Yost SE, Frankel PH, et al. Multi-panel immunofluorescence analysis of tumor infiltrating lymphocytes in triple negative breast cancer: evolution of tumor immune profiles and patient prognosis. *PLoS One* 2020; 15: e0229955. [PubMed: 32150594]
65. Hayashi K, Nogawa D, Kobayashi M, et al. Quantitative high-throughput analysis of tumor infiltrating lymphocytes in breast cancer. *Front Oncol* 2022; 12: 901591.
66. Masugi Y, Abe T, Ueno A, et al. Characterization of spatial distribution of tumor-infiltrating CD8<sup>+</sup> T cells refines their prognostic utility for pancreatic cancer survival. *Mod Pathol* 2019; 32: 1495–1507. [PubMed: 31186528]
67. Yamagami W, Susumu N, Tanaka H, et al. Immunofluorescence-detected infiltration of CD4<sup>+</sup>FOXP3<sup>+</sup> regulatory T cells is relevant to the prognosis of patients with endometrial cancer. *Int J Gynecol Cancer* 2011; 21: 1628–1634. [PubMed: 21897268]
68. Peng H, Wu X, Zhong R, et al. Profiling tumor immune microenvironment of non-small cell lung cancer using multiplex immunofluorescence. *Front Immunol* 2021; 12: 750046.
69. Schalper KA, Brown J, Carvajal-Hausdorf D, et al. Objective measurement and clinical significance of TILs in non-small cell lung cancer. *J Natl Cancer Inst* 2015; 107: dju435.
70. Huang Y-K, Wang M, Sun Y, et al. Macrophage spatial heterogeneity in gastric cancer defined by multiplex immunohistochemistry. *Nat Commun* 2019; 10: 3928. [PubMed: 31477692]
71. Yu Y, Ma X, Zhang Y, et al. Changes in expression of multiple checkpoint molecules and infiltration of tumor immune cells after neoadjuvant chemotherapy in gastric cancer. *J Cancer* 2019; 10: 2754–2763. [PubMed: 31258783]



72. Gide TN, Silva IP, Quek C, et al. Close proximity of immune and tumor cells underlies response to anti-PD-1 based therapies in metastatic melanoma patients. *Oncoimmunology* 2019; 9: 1659093.
73. Wong PF, Wei W, Smithy JW, et al. Multiplex quantitative analysis of tumor-infiltrating lymphocytes and immunotherapy outcome in metastatic melanoma. *Clin Cancer Res* 2019; 8: 2442–2449.
74. Mazzaschi G, Madeddu D, Falco A, et al. Low PD-1 expression in cytotoxic CD8+ tumor-infiltrating lymphocytes confers an immune-privileged tissue microenvironment in NSCLC with a prognostic and predictive value. *Clin Cancer Res* 2018; 24: 407–419. [PubMed: 29074606]
75. Parra ER, Villalobos P, Behrens C, et al. Effect of neoadjuvant chemotherapy on the immune microenvironment in non-small cell lung carcinomas as determined by multiplex immunofluorescence and image analysis approaches. *J Immunother Cancer* 2018; 6: 48. [PubMed: 29871672]
76. Brown JR, Wimberly H, Lannin DR, et al. Multiplexed quantitative analysis of CD3, CD8, and CD20 predicts response to neoadjuvant chemotherapy in breast cancer. *Clin Cancer Res* 2014; 20: 5995–6005. [PubMed: 25255793]
77. De Angelis C, Nagi C, Hoyt CC, et al. Evaluation of the predictive role of tumor immune infiltrate in patients with HER2-positive breast cancer treated with neoadjuvant anti-HER2 therapy without chemotherapy. *Clin Cancer Res* 2020; 26: 738–745. [PubMed: 31653641]
78. Wimberly H, Brown JR, Schalper K, et al. PD-L1 expression correlates with tumor-infiltrating lymphocytes and response to neoadjuvant chemotherapy in breast cancer. *Cancer Immunol Res* 2015; 3: 326–332. [PubMed: 25527356]
79. Chen Y, Jia K, Sun Y, et al. Predicting response to immunotherapy in gastric cancer via multi-dimensional analyses of the tumour immune microenvironment. *Nat Commun* 2022; 13: 4851. [PubMed: 35982052]
80. Liu Y, Zugazagoitia J, Shabbir Ahmed F, et al. Immune cell PD-L1 colocalizes with macrophages and is associated with outcome in PD-1 pathway blockade therapy. *Clin Cancer Res* 2020; 26: 970–977. [PubMed: 31615933]
81. Clemente CG, Mihm MC, Bufalino R, et al. Prognostic value of tumor infiltrating lymphocytes in the vertical growth phase of primary cutaneous melanoma. *Cancer* 1996; 77: 1303–1310. [PubMed: 8608507]
82. Liu F, Lang R, Zhao J, et al. CD8<sup>+</sup> cytotoxic T cell and FOXP3<sup>+</sup> regulatory T cell infiltration in relation to breast cancer survival and molecular subtypes. *Breast Cancer Res Treat* 2011; 130: 645–655. [PubMed: 21717105]
83. Hülsen S, Lippolis E, Ferrazzi F, et al. High stroma T-cell infiltration is associated with better survival in stage pT1 bladder cancer. *Int J Mol Sci* 2020; 21: 8407. [PubMed: 33182484]
84. Menares E, Gálvez-Cacino F, Cáceres-Morgado P, et al. Tissue-resident memory CD8<sup>+</sup> T cells amplify anti-tumor immunity by triggering antigen spreading through dendritic cells. *Nat Commun* 2019; 10: 4401. [PubMed: 31562311]
85. Kmiecik J, Poli A, Brons NHC, et al. Elevated CD3<sup>+</sup> and CD8<sup>+</sup> tumor-infiltrating immune cells correlate with prolonged survival in glioblastoma patients despite integrated immunosuppressive mechanisms in the tumor microenvironment and at the systemic level. *J Neuroimmunol* 2013; 1–2: 71–83.
86. Piersma SJ, Jordanova ES, van Poelgeest MIE, et al. High number of intraepithelial CD8+ tumor-infiltrating lymphocytes is associated with the absence of lymph node metastases in patients with large early-stage cervical cancer. *Cancer Res* 2007; 67: 354–361. [PubMed: 17210718]
87. Maimela NR, Liu S, Zhang Y. Fates of CD8<sup>+</sup> T cells in tumor microenvironment. *Comput Struct Biotechnol J* 2018; 17: 1–13. [PubMed: 30581539]
88. Saleh R, Elkord E. FoxP3<sup>+</sup> T regulatory cells in cancer: prognostic biomarkers and therapeutic targets. *Cancer Lett* 2020; 490: 174–185. [PubMed: 32721551]
89. Tuminello S, Veluswamy R, Lieberman-Cribbin W, et al. Prognostic value of immune cells in the tumor microenvironment of early-stage lung cancer: a meta-analysis. *Oncotarget* 2019; 10: 7142–7155. [PubMed: 31903172]
90. Carstens JL, Correa de Sampaio P, Yang D, et al. Spatial computation of intratumoral T cells correlates with survival of patients with pancreatic cancer. *Nat Commun* 2017; 8: 15095.



91. Yang L, Zhang W, Sun J, et al. Functional status and spatial interaction of T cell subsets driven by specific tumor microenvironment correlate with recurrence of non-small cell lung cancer. *Front Immunol* 2023; 13: 1022638.
92. Tsujikawa T, Mitsuda J, Ogi H, et al. Prognostic significance of spatial immune profiles in human solid cancers. *Cancer Sci* 2020; 111: 3426–3434. [PubMed: 32726495]
93. Nearchou LP, Lillard K, Gavriel CG, et al. Automated analysis of lymphocytic infiltration, tumor budding, and their spatial relationship improves prognostic accuracy in colorectal cancer. *Cancer Immunol Res* 2019; 7: 609–620. [PubMed: 30846441]
94. Banik G, Betts CB, Liudahk SM, et al. High-dimensional multiplexed immunohistochemical characterization of immune contexture in human cancers. *Methods Enzymol* 2020; 635: 1–20. [PubMed: 32122539]
95. Barua S, Fang P, Sharma A, et al. Spatial interaction of tumor cells and regulatory T cells correlates with survival in non-small cell lung cancer. *Lung Cancer* 2018; 117: 73–79. [PubMed: 29409671]
96. Mezheyeuski A, Backman M, Mattsson J, et al. An immune score reflecting pro- and anti-tumoural balance of tumour microenvironment has major prognostic impact and predicts immunotherapy response in solid cancers. *EBioMedicine* 2023; 88: 104452.
97. Werner F, Wagner C, Simon M, et al. A standardized analysis of tertiary lymphoid structures in human melanoma: disease progression- and tumor site-associated changes with germinal center alteration. *Front Immunol* 2021; 12: 675146.
98. Lynch KT, Young SJ, Meneveau MO, et al. Heterogeneity in tertiary lymphoid structure B-cells correlates with patient survival in metastatic melanoma. *J Immunother Cancer* 2021; 9: e002273. [PubMed: 34103353]
99. Dieu-Nosjean M-C, Goc J, Giraldo NA, et al. Tertiary lymphoid structures in cancer and beyond. *Trends Immunol* 2014; 35: 571–580. [PubMed: 25443495]
100. Attrill GH, Ferguson PM, Palendira U, et al. The tumour immune landscape and its implications in cutaneous melanoma. *Pigment Cell Melanoma Res* 2021; 34: 529–549. [PubMed: 32939993]
101. Hersom M, Jørgensen JT. Companion and complementary diagnostics-focus on PD-L1 expression assays for PD-1/PD-L1 checkpoint inhibitors in non-small cell lung cancer. *Ther Drug Monit* 2018; 40: 9–16. [PubMed: 29084031]
102. US Food and Drug Administration. List of cleared or approved companion diagnostic devices (in vitro and imaging tools) |FDA. [Accessed 15 March 2023]. Available from: <https://www.fda.gov/medical-devices/in-vitro-diagnostics/list-cleared-or-approved-companion-diagnostic-devices-in-vitro-and-imaging-tools>
103. Li H, Van Der Merwe PA, Sivakumar S. Biomarkers of response to PD-1 pathway blockade. *Br J Cancer* 2022; 126: 1663–1675. [PubMed: 35228677]
104. Herbst RS, Soria J-C, Kowanetz M, et al. Predictive correlates of response to the anti-PD-L1 antibody MPDL3280A in cancer patients. *Nature* 2014; 515: 563–567. [PubMed: 25428504]
105. Chalabi M, Fanchi LF, Dijkstra KK, et al. Neoadjuvant immunotherapy leads to pathological responses in MMR-proficient and MMR-deficient early-stage colon cancers. *Nat Med* 2020; 26: 566–576. [PubMed: 32251400]
106. de Vries NL, van de Haar J, Veninga V, et al.  $\gamma\delta$  T cells are effectors of immunotherapy in cancers with HLA class I defects. *Nature* 2023; 613: 743–750. [PubMed: 36631610]
107. Tumei PC, Harview CL, Yearley JH, et al. PD-1 blockade induces responses by inhibiting adaptive immune resistance. *Nature* 2014; 515: 568–571. [PubMed: 25428505]
108. Giraldo NA, Nguyen P, Engle EL, et al. Multidimensional, quantitative assessment of PD-1/PD-L1 expression in patients with Merkel cell carcinoma and association with response to pembrolizumab. *J Immunother Cancer* 2018; 6: 99.
109. Chen P-L, Roh W, Reuben A, et al. Analysis of immune signatures in longitudinal tumor samples yields insight into biomarkers of response and mechanisms of resistance to immune checkpoint blockade. *Cancer Discov* 2016; 6: 827–837. [PubMed: 27301722]
110. Anagnostou V, Yarchoan M, Hansen AR, et al. Immuno-oncology trial endpoints: capturing clinically meaningful activity. *Clin Cancer Res* 2017; 23: 4959–1969. [PubMed: 28864724]

111. Denkert C, Loibl S, Noske A, et al. Tumor-associated lymphocytes As an independent predictor of response to neoadjuvant chemotherapy in breast cancer. *J Clin Oncol* 2010; 28: 105–113. [PubMed: 19917869]
112. Chua W, Charles KA, Baracos VE, et al. Neutrophil/lymphocyte ratio predicts chemotherapy outcomes in patients with advanced colorectal cancer. *Br J Cancer* 2011; 104: 1288–1295. [PubMed: 21448173]
113. Vitkin N, Nersesian S, Siemens DR, et al. The tumor immune contexture of prostate cancer. *Front Immunol* 2019; 10: 603. [PubMed: 30984182]
114. Jiang T, Shi T, Zhang H, et al. Tumor neoantigens: from basic research to clinical applications. *J Hematol Oncol* 2019; 12: 93. [PubMed: 31492199]
115. Hou Y, Nitta H, Wei L, et al. Evaluation of immune reaction and PD-L1 expression using multiplex immunohistochemistry in HER2-positive breast cancer: the association with response to anti-HER2 neoadjuvant therapy. *Clin Breast Cancer* 2018; 18: e237–e244. [PubMed: 29198959]
116. Harms PW, Frankel TL, Moutafi M, et al. Multiplex immunohistochemistry and immunofluorescence: a practical update for pathologists. *Mod Pathol* 2023; 36: 100197.
117. Abels E, Pantanowitz L, Aeffner F, et al. Computational pathology definitions, best practices, and recommendations for regulatory guidance: a white paper from the digital pathology association. *J Pathol* 2019; 249: 286–294. [PubMed: 31355445]
118. Tizhoosh HR, Pantanowitz L. Artificial intelligence and digital pathology: challenges and opportunities. *J Pathol Inform* 2018; 9: 38. [PubMed: 30607305]
119. Akturk G, Parra ER, Gjini E, et al. Multiplex tissue imaging harmonization: a multicenter experience from CEVLAC-CIDC immuno-oncology biomarkers network. *Clin Cancer Res* 2021; 27: 5072–5083. [PubMed: 34253580]
120. Agrawal L, Engel KB, Greytak SR, et al. Understanding preanalytical variables and their effects on clinical biomarkers of oncology and immunotherapy. *Semin Cancer Biol* 2018: 26–38.
121. Engel KB, Moore HM. Effects of preanalytical variables on the detection of proteins by immunohistochemistry in formalin-fixed, paraffin-embedded tissue. *Arch Pathol Lab Med* 2011; 135: 537–543. [PubMed: 21526952]
122. Chen HX, Song M, Maecker HT, et al. Network for biomarker immunoprofiling for cancer immunotherapy: cancer immune monitoring and analysis centers and cancer immunologic data commons (CIMAC-CIDC). *Clin Cancer Res* 2021; 27: 5038–5048. [PubMed: 33419780]
123. Taube JM, Roman K, Engle EL, et al. Multi-institutional TSA-amplified multiplexed immunofluorescence reproducibility evaluation (MITRE) study. *J Immunother Cancer* 2021; 9: e002197. [PubMed: 34266881]
124. Bodenmiller B Multiplexed epitope-based tissue imaging for discovery and healthcare applications. *Cell Syst* 2016; 2: 225–238. [PubMed: 27135535]

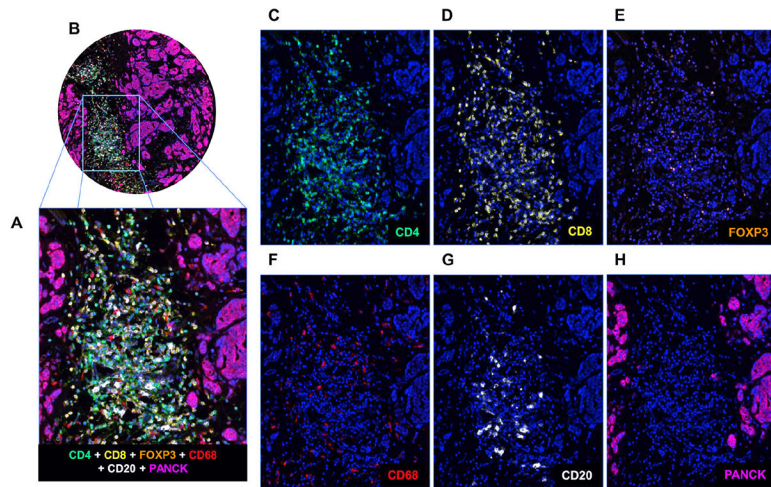


**Figure 1.** mIF staining of a panel of five immune markers plus one epithelial marker. (A and B) A breast cancer TMA core showing composite staining of each of the six markers in the mIF panel (CD4, CD8, F0XP3, CD68, CD68, and PanCK) together with DAPI. (C–H) Individual images of CD4 (green), CD8 (yellow), F0XP3 (orange), CD68 (red), CD20 (white), and PanCK (purple) with DAPI counterstain.

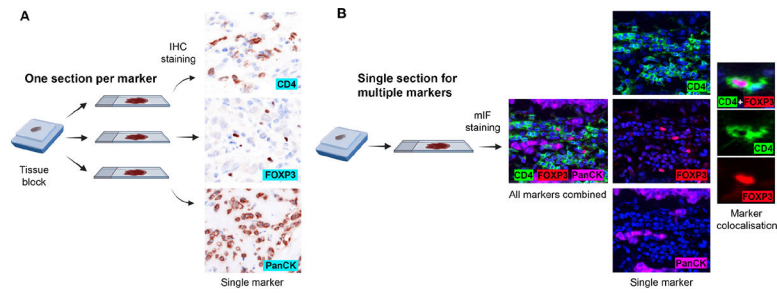


**Figure 2.** Comparison of experimental design between conventional chromogenic IHC and mIF. (A) In conventional chromogenic IHC, each marker requires a separate slide. Although multiplexing with chromogenic IHC is possible, it is severely restricted in terms of the number of markers that can be simultaneously stained. (B) With mIF, one section is enough to examine multiple markers. The figure was partly created using [BioRender.com](https://www.biorender.com).

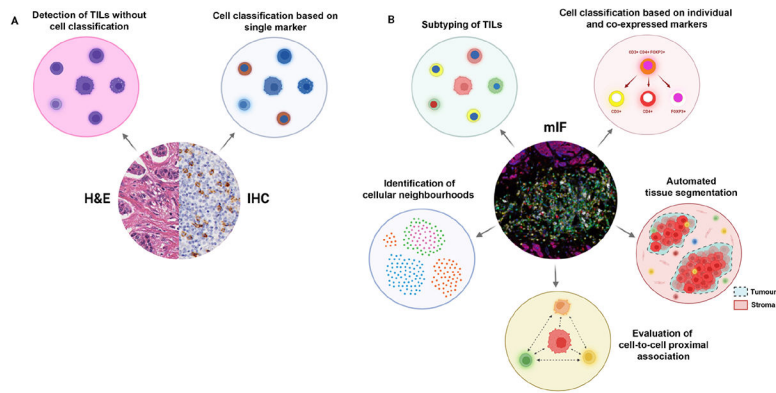


**Figure 3.**

TIL profiling with H&E versus conventional chromogenic IHC versus mIF. (A) H&E staining enables the measurement of total TILs in tissue, whereas, with conventional IHC, a specific immune population can be profiled based on a single protein marker. (B) mIF staining allows the total TIL population to be subtyped based on multiple markers. It is also possible to further characterise cells based on marker colocalisation. With an epithelial or tumour differentiation marker, it is possible to automate tumour-stroma segmentation with image analysis software. Furthermore, multiplex images can be used to map spatial distributions of different cell phenotypes and examine their proximal associations, and further identify distinct cellular neighbourhoods. Created with [BioRender.com](https://www.biorender.com).

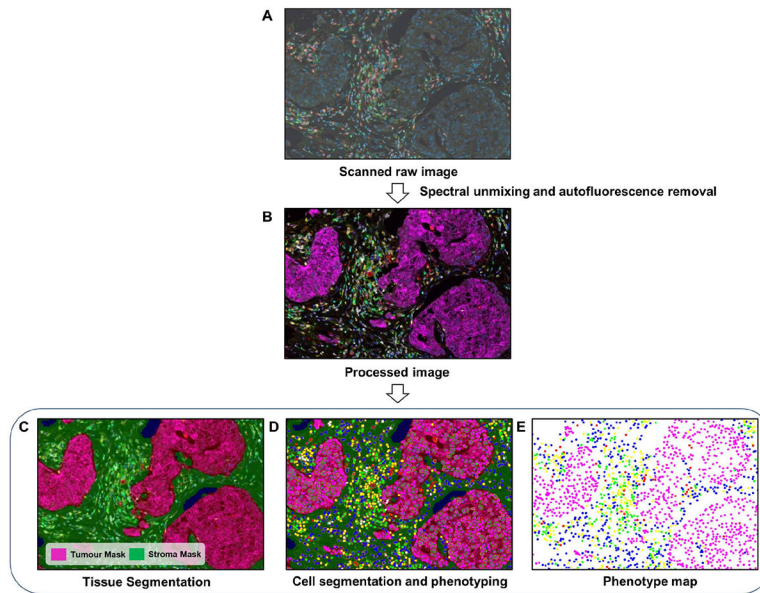


**Figure 4.** DIA workflow for mIF. (A) First, raw images are generated by scanning stained tissue slides. (B) Spectral unmixing and autofluorescence removal are performed with the software to extract the true signals from each marker. (C) A tissue segmentation algorithm is run to segment tumour and stromal areas. (D) Cell segmentation followed by cell phenotyping is performed to classify all cells based on the marker panel used. (E) Finally, spatial mapping of all cell classes is carried out for further proximity analysis. The images were generated using inForm<sup>®</sup> image analysis software, Akoya Bioscience.



**Table 1.**

Application of multiplex staining in clinical immune profiling studies.

Tumour type	Marker panel	Summary	Reference
Prognostic studies			
Breast cancer (HER2+ and TNBC)	CD4, CD8, CD20, FOXP3, CD68, PanCK	Higher B cell infiltration was associated with better overall survival	[62]
Breast cancer	CD8, CD103, CD69, PanCK, DAPI	Higher tissue-resident memory T cell infiltration was associated with better recurrence-free survival	[63]
Breast cancer (TNBC)	CD4, CD8, FOXP3, CD20, CD33, PD-1	Higher PD-1+ CD8+ T cells, PD-1+CD4+ T cells were associated with better prognosis	[64]
Breast cancer (TNBC)	CD4, CD8, FOXP3, PD-1, PD-L1	CD4/PD-L1, CD8/PD-1, and CD8/PD-L1 double-positive TILs were significantly associated with recurrence	[65]
Pancreatic ductal adenocarcinomas	CD8, KRT7	High density of CD8+ T cells in tumour centre was associated with improved survival	[66]
Endometrial cancer	CD8, CD4, FOXP3	High Treg counts and Treg/CD8+ ratios were significantly associated with worse distant metastasis-free survival	[67]
Lung cancer (NSCLC)	Panel 1: CD4, CD38, CD68, FOXP3, CD20 Panel 2: CD8, PD-L1, CD163, CD68, CD133	Patients were classified into three subtypes based on their unique immune composition (immune activated, immune defected and immune exempted), where immune-activated patients showed the longest disease-free survival	[68]
Lung cancer (NSCLC)	CD3, CD8, CD20	Higher CD3+ and CD8+ infiltration was associated with better outcome	[69]
Gastric cancer	CD68, CD163, CD206, IRF8, PD-L1	Higher CD163+ (CD206+) tumour-associated macrophage density with high CD68 expression was associated with better patient survival	[70]
Gastric cancer	CD4, CD8, FOXP3, PD-1, PD-L1, TIM3	Higher levels of CD8, PD-1, and PD-L1 following NAC were associated with better overall survival	[71]
Predictive studies			
Melanoma	CD8, FOXP3, SOX10 PD-1, PD-L1	CD8+ cells within 20 µm of a melanoma cell were predictive of PD-1-based immunotherapy.	[72]
Melanoma	CD4, CD8, CD20, CD3, GZMB, Ki67	Pretreatment lymphocytic infiltration (CD3, CD8) was indicative of anti-PD-1 response	[73]
Lung cancer (NSCLC)	CD3, CD8, CD4, PD-1, CD57, FOXP3, CD25, Granzyme B	CD8+ T cells lacking PD-1 inhibitory receptor positively impacted nivolumab-treated patient survival	[74]
Lung cancer (NSCLC)	Panel 1 - AE1/AE3, PD-L1, CD3, CD4, CD8, and CD68 Panel 2 - AE1/AE3, PD-1, granzyme B, FOXP3, CD45RO, CD57.	Higher intratumoural T helper cell and macrophage levels were associated with chemotherapy outcome	[75]
Breast cancer	CD3, CD20, CD8	CD3, CD8, and CD20 infiltration were predictive of NAC response	[76]
Breast cancer (HER2+)	CD8, CD4, CD20, CD68, FoxP3, CK	CD4+, CD8+, CD20+ s-TILs, CD20+ s-TILs were independently associated with higher pCR in patients treated with neoadjuvant anti-HER2 therapy	[77]
Breast cancer	PD-L1, PanCK	PD-L1 was predictive of NAC response	[78]
Gastric cancer	CD8, PD-1, PD-L1, TIM-3, LAG-3, CD4, CD20, FoxP3, CTLA-4, CD68, CD163, CD66b, HLA-DR, STING	Multi-marker protein signature predicts anti-PD-1/PD-L1 therapy response	[79]

Author Manuscript

Author Manuscript

Author Manuscript

Author Manuscript

Tumour type	Marker panel	Summary	Reference
Lung cancer (NSCLC)	PD-L1, CD68, CD8	High level of PD-1 in macrophages was linked with higher CD8 <sup>+</sup> cell infiltration and better survival outcome in PD-1 pathway blockade therapy	[80]

pCR, pathological complete response; s-TIL, stromal tumour-infiltrating lymphocyte; TNBC, triple-negative breast cancer.